Article

Molecular Cell

Cancer/Testis Antigen PASD1 Silences the Circadian Clock

Graphical Abstract

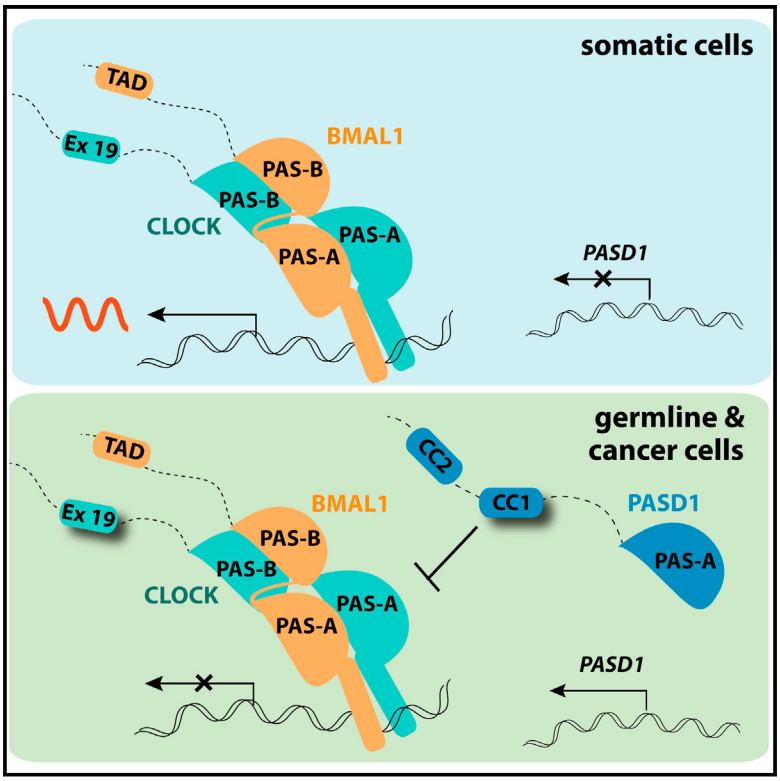

Highlights

- PASD1 is evolutionarily related to the circadian transcription factor subunit CLOCK
- PASD1 is a nuclear protein that inhibits the transcriptional activity of CLOCK:BMAL1
- Regulation of CLOCK:BMAL1 by PASD1 is functionally linked to CLOCK exon 19
- Downregulation of PASD1 improves amplitude of cycling in human cancer cells

Authors

Alicia K. Michael, Stacy L. Harvey, ..., Alison H. Banham, Carrie L. Partch

Correspondence

cpartch@ucsc.edu

In Brief

The circadian clock orchestrates global changes in transcriptional regulation on a daily basis via the bHLH-PAS transcription factor CLOCK:BMAL1. Michael et al. report that the cancer/testis antigen PASD1 is evolutionarily related to CLOCK and inhibits CLOCK:BMAL1 activity in human cancer.

Michael et al., 2015, Molecular Cell *58*, 743–754
June 4, 2015
http://dx.doi.org/10.1016/j.molcel.2015.03.031

Molecular Cell
Article

Cancer/Testis Antigen PASD1 Silences the Circadian Clock

Alicia K. Michael,[1] Stacy L. Harvey,[1] Patrick J. Sammons,[1] Amanda P. Anderson,[2] Hema M. Kopalle,[1] Alison H. Banham,[2] and Carrie L. Partch[1,3,*]
[1]Department of Chemistry and Biochemistry, University of California, Santa Cruz, Santa Cruz, CA 95064, USA
[2]Nuffield Division of Clinical Laboratory Sciences, Radcliffe Department of Medicine, University of Oxford, Oxford OX3 9DU, UK
[3]Center for Circadian Biology, University of California, San Diego, San Diego, CA 92093, USA
*Correspondence: cpartch@ucsc.edu
http://dx.doi.org/10.1016/j.molcel.2015.03.031

SUMMARY

The circadian clock orchestrates global changes in transcriptional regulation on a daily basis via the bHLH-PAS transcription factor CLOCK:BMAL1. Pathways driven by other bHLH-PAS transcription factors have a homologous repressor that modulates activity on a tissue-specific basis, but none have been identified for CLOCK:BMAL1. We show here that the cancer/testis antigen PASD1 fulfills this role to suppress circadian rhythms. PASD1 is evolutionarily related to CLOCK and interacts with the CLOCK:BMAL1 complex to repress transcriptional activation. Expression of PASD1 is restricted to germline tissues in healthy individuals but can be induced in cells of somatic origin upon oncogenic transformation. Reducing PASD1 in human cancer cells significantly increases the amplitude of transcriptional oscillations to generate more robust circadian rhythms. Our results describe a function for a germline-specific protein in regulation of the circadian clock and provide a molecular link from oncogenic transformation to suppression of circadian rhythms.

INTRODUCTION

The circadian clock coordinates temporal control of physiology by regulating the expression of at least 40% of the genome on a daily basis (Zhang et al., 2014). Disruption of circadian rhythms through environmental stimuli (e.g., light at night) or genetic means can lead to the onset of diseases such as diabetes, cardiovascular disease, premature aging, and cancer (Filipski and Lévi, 2009; Jeyaraj et al., 2012; Kondratov et al., 2006; Marcheva et al., 2010). Understanding the molecular basis of circadian transcriptional regulation in health and disease states offers the opportunity to control vast transcriptional programs that promote health and well-being (Takahashi et al., 2008).

The heterodimeric basic helix-loop-helix PER-ARNT-SIM (bHLH-PAS) transcription factor CLOCK:BMAL1 sits at the core of the molecular circadian clock in mammals. CLOCK:BMAL1 drives expression of core clock factors *Period* (*Per*) and *Cryptochrome* (*Cry*), as well as thousands of additional clock-controlled output genes (Koike et al., 2012; Zhang et al., 2014). PER and CRY complexes interact with CLOCK:BMAL1 in the nucleus to inhibit transcriptional activation and close the feedback loop, generating intrinsic ~24 hr timing (Gustafson and Partch, 2014; Koike et al., 2012; Lee et al., 2001). This cell-autonomous molecular oscillator is present in nearly every mammalian tissue (Nagoshi et al., 2004; Welsh et al., 2004; Yoo et al., 2004) and is regulated by tissue-specific factors to fine-tune circadian output genes according to cell type (Panda et al., 2002; Storch et al., 2002). Although the molecular circadian clock is broadly recognized as a systemic transcriptional regulator, factors that provide tissue-specific regulation of the clock and its outputs remain to be elucidated.

CLOCK and BMAL1 belong to the bHLH-PAS family of transcription factors, which share similar domain architecture but regulate diverse processes, including adaptation to hypoxia, xenobiotic metabolism, and neuronal development (Crews, 1998; Ema et al., 1996; Gu et al., 1998; Mimura et al., 1999). Homotypic interactions between N-terminal DNA-binding bHLH domains and tandem PAS domains guide formation of specific heterodimeric transcription factor complexes (Huang et al., 2012; Scheuermann et al., 2009; Wang et al., 2013). By contrast, bHLH-PAS C termini interact with regulatory factors that modulate activity of the complexes (Freedman et al., 2002; Kobayashi et al., 1997). In CLOCK:BMAL1, the BMAL1 C terminus harbors the essential transactivation domain (TAD) that recruits coactivators CBP/p300 and cryptochrome repressors (Czarna et al., 2011; Kiyohara et al., 2006; Takahata et al., 2000), and a short helical region encoded by CLOCK exon 19 interacts with the histone methyltransferase MLL1 and a vertebrate-specific repressor, CIPC (Katada and Sassone-Corsi, 2010; Zhao et al., 2007). Deletion of exon 19 prevents proper chromatin targeting of CLOCK:BMAL1 to interfere with circadian transcriptional regulation (Gekakis et al., 1998; Vitaterna et al., 2006).

One interesting feature shared by bHLH-PAS transcription factors is their regulation by paralogous PAS domain-containing repressors. By definition, each paralog repressor shares significant homology with an activator subunit, but either possesses a repressive domain and/or lacks a domain(s) necessary for activation (Ema et al., 1996; Evans et al., 2008; Makino et al., 2001; Teh et al., 2006). These repressors are often expressed in a highly restricted manner to control the tissue specificity of

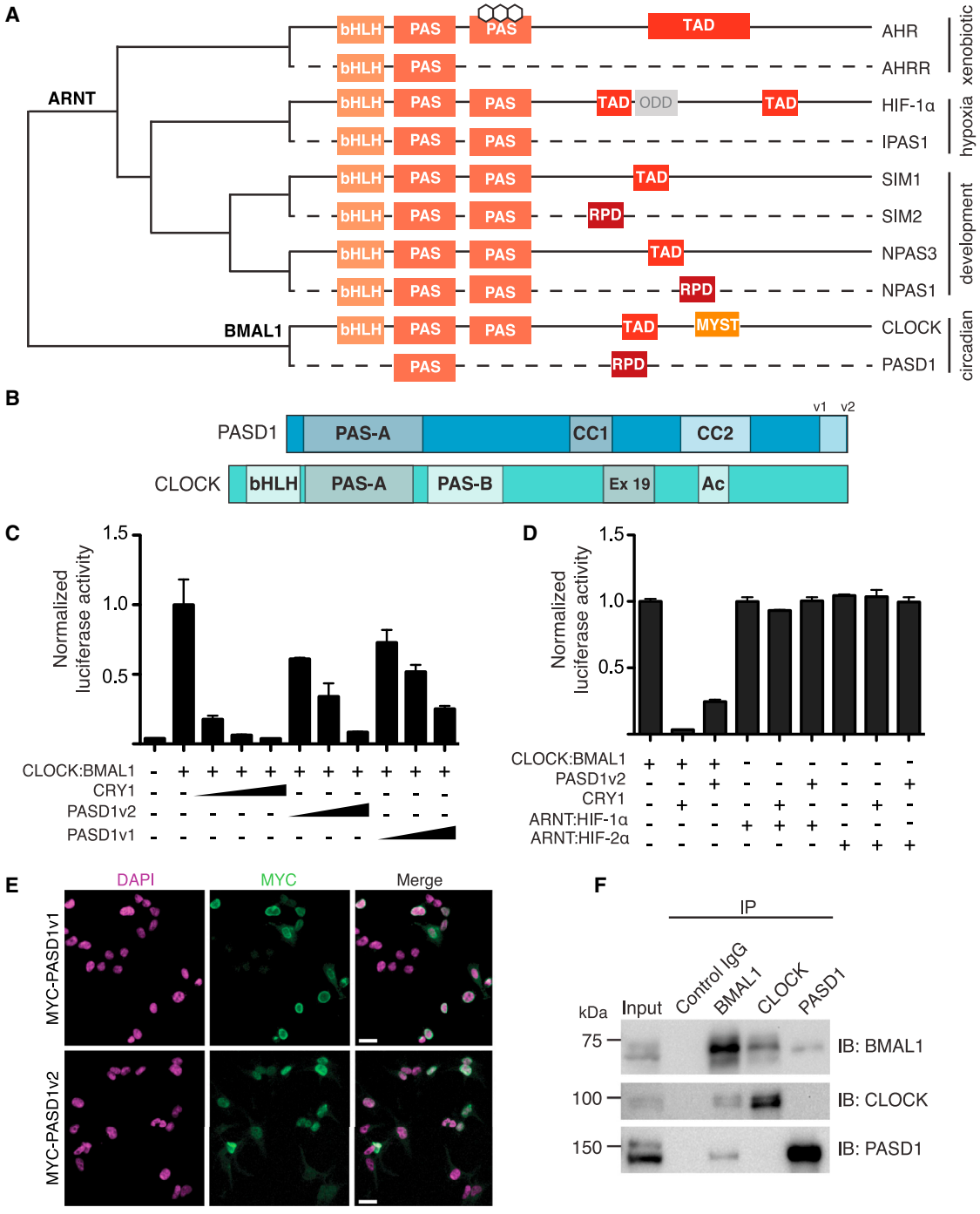

Figure 1. Identification of a Novel Circadian Repressor that Is Homologous to CLOCK

(A) Cladogram of bHLH-PAS transcription factors showing their evolutionary relationship. Each branch of transcription factors within the bHLH-PAS family has a truncated transcriptional repressor that clusters with its related activator subunit and shares similar domain architecture. MYST, histone acetyltransferase motif from the MYST family (Doi et al., 2006); ODD, oxygen-dependent degradation domain; RPD, repression domain; TAD, transactivation domain. The cladogram was generated using EMBL-EBI Clustal Omega. Activator subunits have solid lines; repressors have dashed lines.

(B) Comparison of human PASD1 and CLOCK domain organization. Gray shading highlights regions of high sequence identity with PASD1. Ac, histone acetyltransferase motif; Ex 19, exon 19. v1 and v2 refer to splice isoforms. See also Figure S1A.

(C) Both isoforms of PASD1 inhibit CLOCK:BMAL1 activity in *Per1:luc* reporter gene assays. HEK293T cells were transfected with *Per1:luc*, CLOCK, BMAL1, and increasing amounts of CRY1 or PASD1 plasmid as indicated (n = 3 experiments, mean ± SD).

(legend continued on next page)

transcriptional outputs (Fan et al., 1996; Yamamoto et al., 2004). However, the mechanisms by which the pathway-specific paralogs repress transcriptional activation by their cognate heterodimers and, importantly, how their homology to activator subunits is used to impinge on transcriptional regulation are not well understood.

The dedicated bHLH-PAS family repressor for circadian rhythms has not yet been identified. Here we show that the protein PAS domain containing protein 1 (PASD1) is evolutionarily related to the circadian transcription factor subunit CLOCK and interacts with the CLOCK:BMAL1 complex to inhibit transcriptional activation and suppress circadian timekeeping. Furthermore, deletion of one region, highly conserved with CLOCK exon 19, alleviates repression by PASD1 to suggest that it uses molecular mimicry to interfere with CLOCK:BMAL1 function. As a cancer/testis antigen, expression of PASD1 is natively restricted to gametogenic tissues but can be upregulated in somatic tissues as a consequence of oncogenic transformation. Our work suggests that mechanisms to suppress circadian cycling can be hard-wired in a tissue-specific manner, and we show here that they can be co-opted in cancer cells to attenuate clock function.

RESULTS

Identification of a CLOCK Paralog in Humans

The absence of a paralogous repressor for CLOCK:BMAL1 prompted us to search for human clock protein paralogs that might serve this purpose. Using a PAS domain-based query with the SMART algorithm (Letunic et al., 2015; Schultz et al., 1998), we discovered an uncharacterized PAS domain-containing protein in humans, PASD1, that is homologous to CLOCK (Figures 1A and S1A). In contrast to CLOCK, PASD1 lacks the DNA-binding bHLH domain and the PAS-B domain, both of which are needed to interact with BMAL1 to form a functional heterodimeric transcription factor (Huang et al., 2012). Similarity between PASD1 and CLOCK is restricted to the PAS-A domain and a helical region in the C terminus (Figures 1B and S1A) defined by CLOCK exon 19, which is essential for CLOCK:BMAL1 function (Gekakis et al., 1998; Katada and Sassone-Corsi, 2010; King et al., 1997). *PASD1* has two splice isoforms (*PASD1v1* and *PASD1v2*) that differ only by extension of the C terminus (Figure 1B) (Liggins et al., 2004). The C terminus of PASD1 has more predicted secondary structure than CLOCK, with two conserved helical regions designated coiled coil 1 (CC1) and coiled coil 2 (CC2) (Figure 1B). On the basis of these sequence analyses, PASD1 demonstrates two key properties of a pathway-specific bHLH-PAS repressor: homology to a bHLH-PAS activator subunit with the loss of domain(s) critical for transcriptional activation (Makino et al., 2001; Mimura et al., 1999; Moffett et al., 1997).

PASD1 is an X-linked gene that is broadly conserved in mammals but absent in murine lineages (Figure S1B), a property common to X-linked genes involved in spermatogenesis (Mueller et al., 2013). In healthy individuals, PASD1 is expressed only in germline tissues such as the testis (Djureinovic et al., 2014); however, PASD1 can be found in somatic tissues upon oncogenic transformation (Ait-Tahar et al., 2009; Cooper et al., 2006; Liggins et al., 2004). PASD1 is therefore designated as a cancer/testis antigen, a classification shared with a large family of proteins that are normally expressed only in the germline and whose expression can provoke immune responses when aberrantly upregulated in neoplastic somatic cells (Ait-Tahar et al., 2009; Liggins et al., 2004; Whitehurst, 2014). Although the immunogenicity and expression of PASD1 in a diverse array of human cancers have been well characterized (Joseph-Pietras et al., 2010; Liggins et al., 2010), the cellular function of this protein remains unknown. These data prompted us to investigate whether PASD1 could represent the dedicated bHLH-PAS family repressor that negatively regulates CLOCK:BMAL1.

PASD1 Is a Nuclear Protein that Represses Transcriptional Activation by CLOCK:BMAL1

To determine if PASD1 regulates CLOCK:BMAL1 activity, we conducted a reporter gene assay in HEK293T cells using the *Per1:luc* luciferase reporter (Gekakis et al., 1998). PASD1 had no effect on the *Per1:luc* reporter by itself or in combination with either CLOCK or BMAL1 alone, indicating that it cannot drive transcriptional activation (Figure S2). Titration of either splice isoform of PASD1 led to dose-dependent repression of CLOCK:BMAL1 activity, similar to the core clock repressor cryptochrome 1 (Figure 1C). Furthermore, both CRY1 and PASD1 demonstrated specificity for CLOCK:BMAL1, as co-expression of either repressor with bHLH-PAS homologs HIF-1α:ARNT or HIF-2α:ARNT had no effect on their transcriptional activation of a hypoxia response element from *VEGF* (Figure 1D).

Regulation of CLOCK:BMAL1 transcriptional activity is likely to occur in the nucleus where the complex is localized. To determine the subcellular localization of PASD1, we transfected HEK293T cells with MYC-tagged versions of both splice isoforms of PASD1 and used immunofluorescence to visualize PASD1. Both MYC-tagged PASD1 splice isoforms are localized exclusively in the nucleus, predominantly at the periphery where heterochromatin is generally compartmentalized in metazoan cells (Padeken and Heun, 2014) (Figure 1E). To determine if PASD1 interacts with CLOCK:BMAL1, we performed co-immunoprecipitations of each protein from nuclear lysate of a U2OS cell line stably expressing PASD1-GFP. Endogenous BMAL1 precipitated both CLOCK and PASD1-GFP, while CLOCK precipitated low levels of BMAL1 but no detectable PASD1-GFP (Figure 1F). PASD1-GFP precipitated BMAL1 but not CLOCK, suggesting that PASD1 may target the CLOCK:BMAL1

(D) CRY1 and PASD1 do not inhibit transactivation of a *VEGF:luc* reporter by the bHLH-PAS homologs HIF-1α:ARNT or HIF-2α:ARNT. HA-tagged P1P2N mutants stabilize expression of HIF-1α or HIF-2α under normoxic conditions (Dioum et al., 2009) (n = 3 replicates, mean ± SD).

(E) HEK293T cells were transiently transfected with MYC-PASD1v1 and MYC-PASD1v2, and subcellular localization was determined by immunofluorescence. The scale bar represents 20 μm.

(F) Co-immunoprecipitation of endogenous BMAL1, CLOCK with PASD1-GFP from U2OS *Per2:dluc* PASD1-GFP cells.

See also Figure S1.

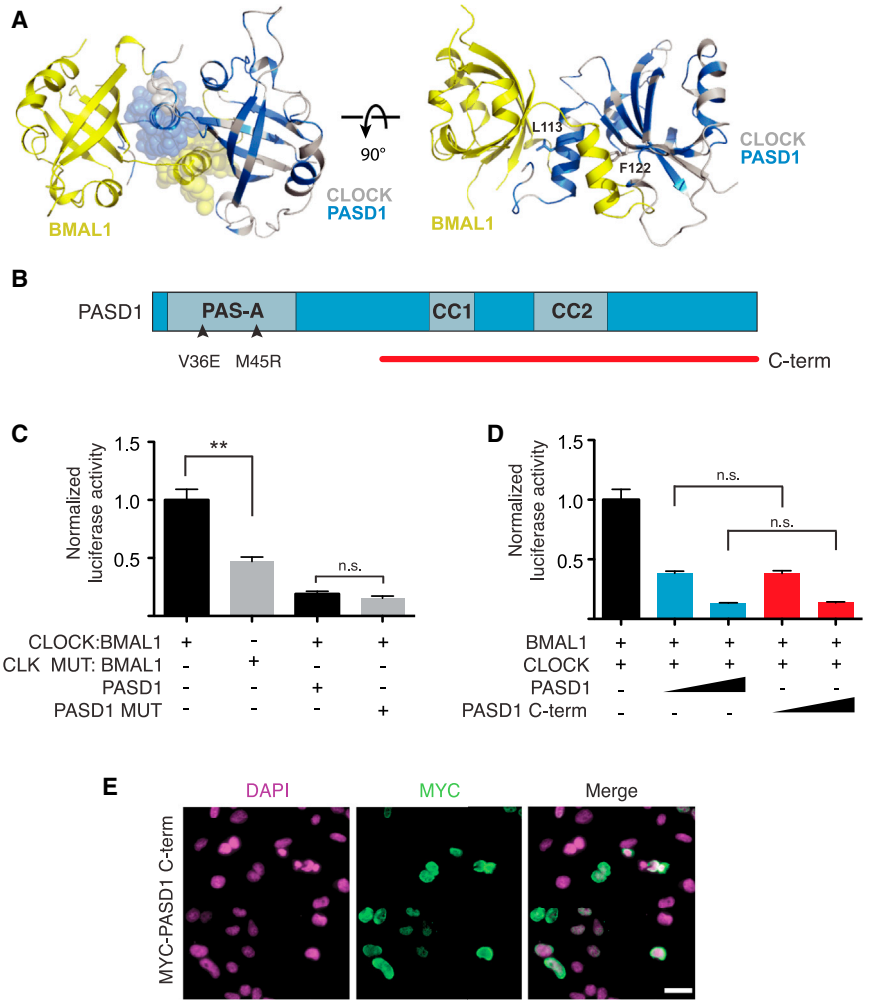

Figure 2. The C Terminus of PASD1 Is Sufficient to Repress CLOCK:BMAL1

(A) Mapping of residues conserved between PASD1 and CLOCK onto the CLOCK:BMAL1 PAS-A domain interface (PDB: 4F3L). BMAL1 (yellow), CLOCK residues conserved with PASD1 (blue) or non-conserved (white). Location of the CLOCK PAS-A mutations (L113E/F122R) that disrupt the CLOCK:BMAL1 heterodimer and reduce transactivation are shown (Huang et al., 2012).

(B) Schematic of PASD1 expression constructs. Arrowheads indicate point mutations in the PAS-A domain.

(C) Mutation of the PASD1 PAS-A β sheet interface (V36E/M45R) does not affect repression of CLOCK:BMAL1, while mutation of analogous residues in the PAS-A domain of CLOCK (L113E/F122R) reduces activation of the *Per1:luc* gene (Huang et al., 2012) (n = 3 experiments, mean ± SD). Significance was determined by Student's t test: $^{**}p < 0.01$.

(D) The PASD1 C terminus is sufficient to repress CLOCK:BMAL1 *Per1:luc* luciferase expression (n = 3 replicates, mean ± SD). Significance was determined by Student's t test.

(E) HEK293T cells were transiently transfected with MYC-PASD1v1 C-term and subcellular localization was determined by immunofluorescence. The scale bar represents 20 μm.

See also Figure S2.

complex through interaction with BMAL1. Taken together, these data show that PASD1 is a potent and specific nuclear repressor of the CLOCK:BMAL1 complex.

Identification of the PASD1 Repressive Domain

To understand how PASD1 regulates CLOCK:BMAL1 activity, we set out to identify the repressive domain on PASD1. We initially focused our attention on the PASD1 PAS-A domain because it shares a high degree of conservation with CLOCK (Figure S1A). Moreover, PASD1 residues conserved with CLOCK are predominantly localized at the PAS-A interface of the CLOCK:BMAL1 heterodimer (Figure 2A). Mutations in CLOCK PAS-A (L113E/F122R) at this interface diminish interaction with BMAL1 and decrease transactivation by the complex in the *Per1:luc* reporter assay (Huang et al., 2012). We reasoned that if PASD1 represses CLOCK:BMAL1 by sequestration of the BMAL1 PAS-A domain, then mutation of homologous residues in PASD1 (V36E/M45R) should reduce inhibition of CLOCK:BMAL1 by disrupting the interaction (Figure 2B). The CLOCK PAS-A L113E/F122R mutant caused a significant decrease in *Per1:luc* activation with BMAL1, as previously reported (Huang et al., 2012), but we saw no effect of the PAS-A V36E/M45R mutation on the ability of PASD1 to repress CLOCK:BMAL1 (Figure 2C). Moreover, we determined that both full-length PASD1 and the isolated C terminus repressed CLOCK:BMAL1 activity to the same degree (Figure 2D) and localized to the nucleus (Figure 2E), demonstrating that the PASD1 C terminus is sufficient to repress CLOCK:BMAL1 activity.

The other major region of conservation between PASD1 and CLOCK exists within the coiled-coil domain 1 (CC1) in the C terminus of PASD1, which exhibits significant homology with exon 19 of CLOCK (Figure 3A). This short helical region of CLOCK is important for transcriptional activation and necessary to sustain a robust amplitude of cycling (Gekakis et al., 1998; Katada and Sassone-Corsi, 2010; Vitaterna et al., 2006), suggesting that its conservation within PASD1 might play a role in its regulation of CLOCK:BMAL1 activity. We deleted the CC1 region from the full-length protein (PASD1ΔCC1) or the isolated C terminus (C-term ΔCC1) to probe its role in CLOCK:BMAL1 regulation (Figure 3B). Although CC1-truncated forms of PASD1 retained nuclear localization and were expressed to the degree as full-length protein (Figures 3C and S3A), repression of CLOCK:BMAL1-driven luciferase activity was significantly impaired (Figure 3D). Co-expression of CLOCK and BMAL1 drives their nuclear localization (Kondratov et al., 2003; Kwon et al., 2006). Full-length PASD1 and the C terminus both interacted with co-expressed CLOCK and BMAL1, and complex formation was visibly reduced with deletion of CC1 (Figures 3E and S3B).

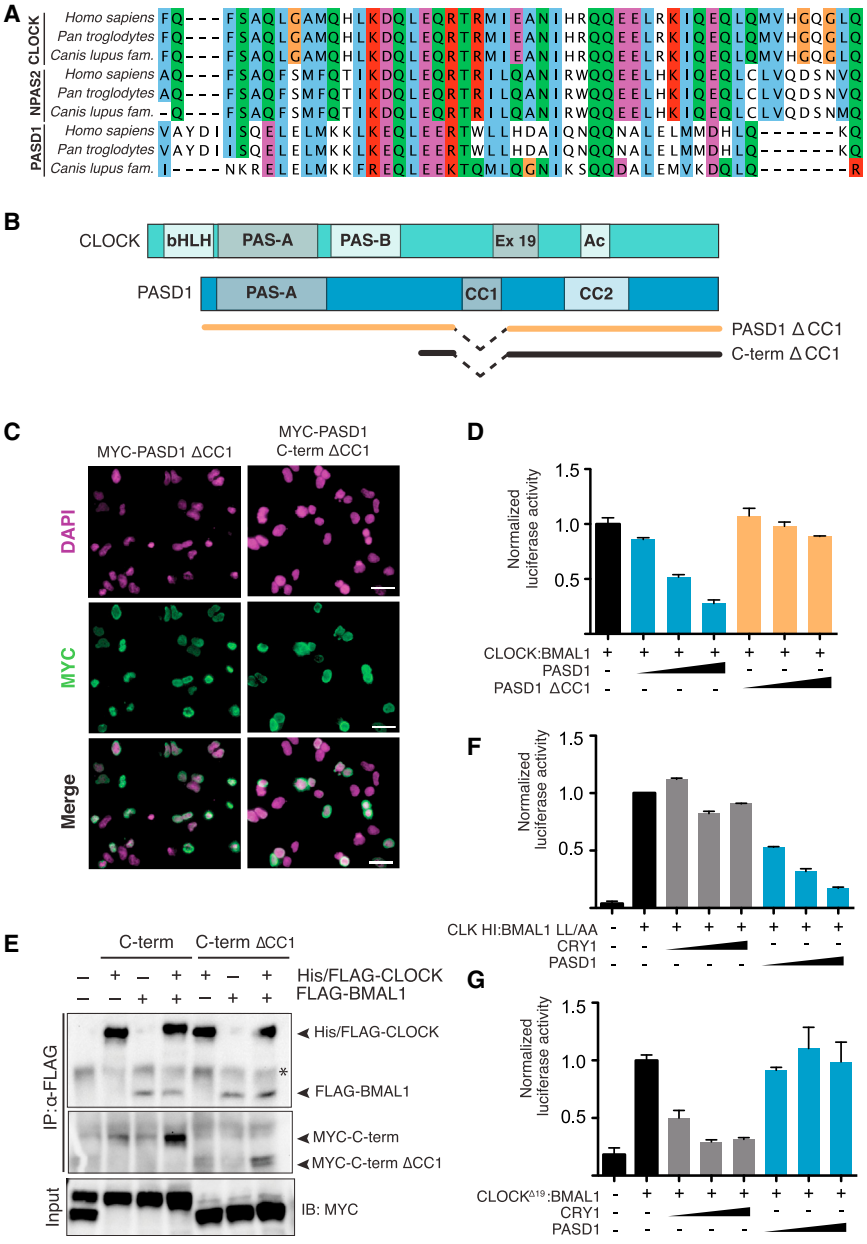

Figure 3. PASD1 Requires Its CC1 Domain and Exon 19 of CLOCK to Repress CLOCK:BMAL1

(A) TCoffee alignment of CLOCK and NPAS2 exon 19 with PASD1 CC1 domain.

(B) Schematic of PASD1 expression constructs used in luciferase assays.

(C) Deletion of CC1 domain in the full-length protein or C terminus does not affect nuclear localization. HEK293T cells were transfected with MYC-tagged constructs, and subcellular localization was visualized by immunofluorescence. The scale bar represents 20 μm.

(D) Deletion of the PASD1 CC1 domain (residues 365–415) relieves repression of CLOCK:BMAL1 activation of the *Per1:luc* gene (n = 3 experiments, mean ± SD). See also Figure S3A.

(E) PASD1-MYC tagged C-term ΔCC1 shows decreased interaction when both CLOCK and BMAL1 are precipitated compared with the MYC tagged C terminus. Asterisk denotes non-specific protein. See also Figure S3B.

(F) Mutation of two residues in the PAS-B domain HI loop of CLOCK (Q361P/W362R; HI) and BMAL1 (L606A/L607A; LL/AA) that reduce repression by CRY1 do not affect PASD1-mediated repression in *Per1:luc* luciferase assays (n = 3 replicates, mean ± SD).

(G) CRY1 can inhibit transactivation by CLOCK$^{\Delta 19}$:BMAL1, but PASD1 cannot (n = 3 replicates, mean ± SD).

See also Figure S3.

Therefore, the CC1 domain of PASD1 is important for interaction with its cognate transcription factor and transcriptional repression.

Regulation of CLOCK:BMAL1 by PASD1 CC1 and CLOCK Exon 19 Are Functionally Linked

To probe how PASD1 impinges on transcriptional activation by CLOCK:BMAL1, we tested two transcription factor mutants that interfere discretely with two key regulatory domains on CLOCK:BMAL1: the BMAL1 TAD or CLOCK exon 19. Both CLOCK:BMAL1 mutants had reduced activity relative to wild-type CLOCK:BMAL1, but overall activity of the heterodimer was sufficiently robust (~3- to 4-fold activation of the *Per1:luc* reporter over background) to probe regulation of the complexes (Figure S3C). We first tested the CLOCK HI:BMAL1 LL/AA mutant, which interferes with sequestration of the BMAL1 TAD by CRY1 (Xu et al., 2015). Although the CLOCK HI:BMAL1 LL/AA mutant abolished repression by CRY1, PASD1 still potently repressed transcriptional activation to suggest that PASD1 does not inhibit CLOCK:BMAL1 through sequestration of the BMAL1 TAD (Figure 3F). We then tested the ability of PASD1 to repress CLOCK$^{\Delta 19}$:BMAL1, which lacks the 51 amino acids encoded by exon 19 (Gekakis et al., 1998; King et al., 1997). CRY1 could still potently repress the residual transactivation potential in the CLOCK$^{\Delta 19}$:BMAL1 mutant (Figure 3G); however, PASD1 could no longer exhibited repression of CLOCK$^{\Delta 19}$:BMAL1 activity. We interpret these data to mean that PASD1 interferes with CLOCK:BMAL1 function in a manner that depends on the activating potential of exon 19; once disrupted in the CLOCK$^{\Delta 19}$:BMAL1 mutant, PASD1 can no longer further repress the heterodimer.

PASD1 Suppresses Circadian Cycling

To determine the effect of PASD1 expression on intact molecular circadian oscillators, we examined circadian cycling in mouse NIH 3T3 fibroblast cells, which completely lack the *PASD1* gene, and human U2OS osteosarcoma cells that cycle with

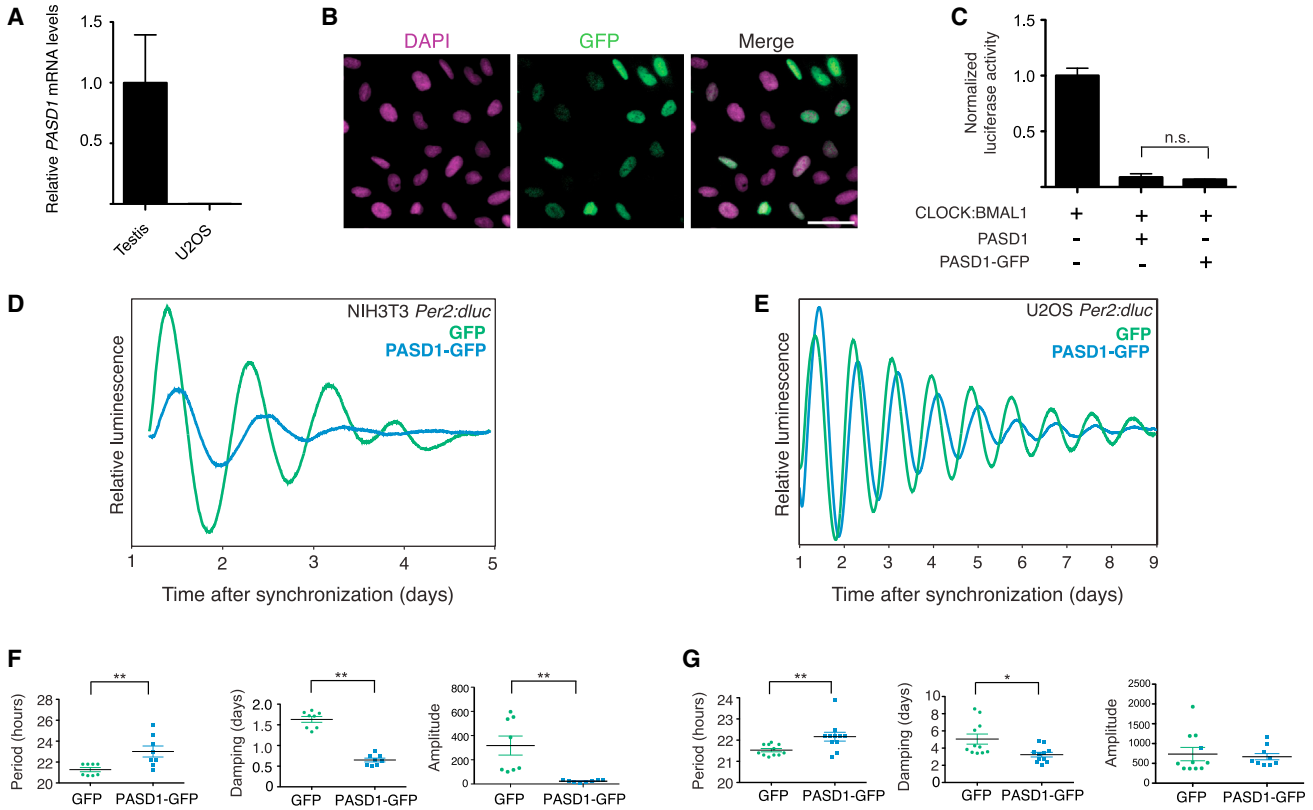

Figure 4. Overexpression of PASD1 Lengthens Period and Increases Damping of Circadian Cycling in Cell Culture

(A) Comparison of *PASD1* expression in human testis and U2OS cells by RT-qPCR (n = 3 replicates, mean ± SEM). See also Figure S4A.

(B) Immunofluorescence of PASD1-GFP in a U2OS *Per2:dluc* cell line stably expressing PASD1-GFP. The scale bar represents 20 μm. See also Figure S4B.

(C) Fusion of GFP to PASD1 does not affect repression of CLOCK:BMAL1 (n = 3 replicates, mean ± SD). Significance was determined by Student's t test.

(D) Representative bioluminescence records from mouse NIH 3T3 *Per2:dluc* cells expressing GFP or PASD1-GFP (n = 8).

(E) Representative bioluminescence records from human U2OS *Per2:dluc* cells expressing GFP or PASD1-GFP (n = 11).

(F) PASD1-GFP expression in NIH 3T3 *Per2:dluc* cells significantly lengthens period, increases damping rate and decreases amplitude. Period (hours) ± SEM: GFP 21.3 ± 0.2, PASD1-GFP 23.0 ± 0.53. Damping (days) ± SEM: GFP 1.29 ± 0.3, PASD1-GFP 0.65 ± 0.046 (n = 8 replicates, mean ± SEM).

(G) PASD1-GFP expression in U2OS *Per2:dluc* cells significantly lengthens period and increases damping rate. Period (hours) ± SEM: GFP 21.55 ± 0.07, PASD1-GFP 22.2 ± 0.2. Damping (days) ± SEM: GFP 5.05 ± 0.6, PASD1-GFP 3.24 ± 0.27 (n = 11 replicates, mean ± SEM). Significance was determined by Student's t test: *p < 0.05; **p < 0.01.

See also Figure S4.

high amplitude (Hirota et al., 2008; Vollmers et al., 2008) but do not express *PASD1* as determined by RT-qPCR (Figures 4A and S4A). We generated *Per2:dluc* reporter cell lines stably expressing PASD1-GFP or a GFP control after determining that GFP fusion does not alter PASD1 subcellular localization or attenuate PASD1 activity toward CLOCK:BMAL1 (Figures 4B, 4C, and S4B). In both lines, expression of PASD1-GFP led to significant alterations in the molecular oscillator (Figures 4D and 4E), marked by increases in the period (~1 h) and rate of damping (Figures 4F and 4G), which indicates defects in cell-autonomous clocks that lead to desynchronization of the population (Izumo et al., 2006). In mouse NIH 3T3 fibroblasts, we also noted a significant decrease in amplitude upon PASD1-GFP expression that was not as pronounced in U2OS cells, which could be attributable to the higher basal amplitude of cycling in the U2OS cell line (Figures 4F and 4G). Collectively, these findings demonstrate that introduction of PASD1 into naive cells attenuates the robustness of the molecular circadian oscillator.

Identification of PASD1-Positive Cancer Cell Lines

PASD1 is not expressed in cells of somatic origin unless it has been de-repressed because of malignant transformation (Kim et al., 2013). The circadian clock is frequently disrupted in cancer, allowing cells to escape its daily temporal control of regulated processes and facilitate tumor growth (Filipski and Lévi, 2009; Sahar and Sassone-Corsi, 2009; Takahashi et al., 2008). To determine if upregulation of PASD1 influences the robustness of the circadian clock in human cancer, we screened a panel of cancer cell lines by examining mRNA and protein expression of the two *PASD1* splice isoforms. TaqMan probes common to both splice isoforms (exons 11 and 12) or specific for the longer *PASD1v2* isoform (exons 14 and 15) reported similar levels of expression, indicating that the longer isoform is predominantly

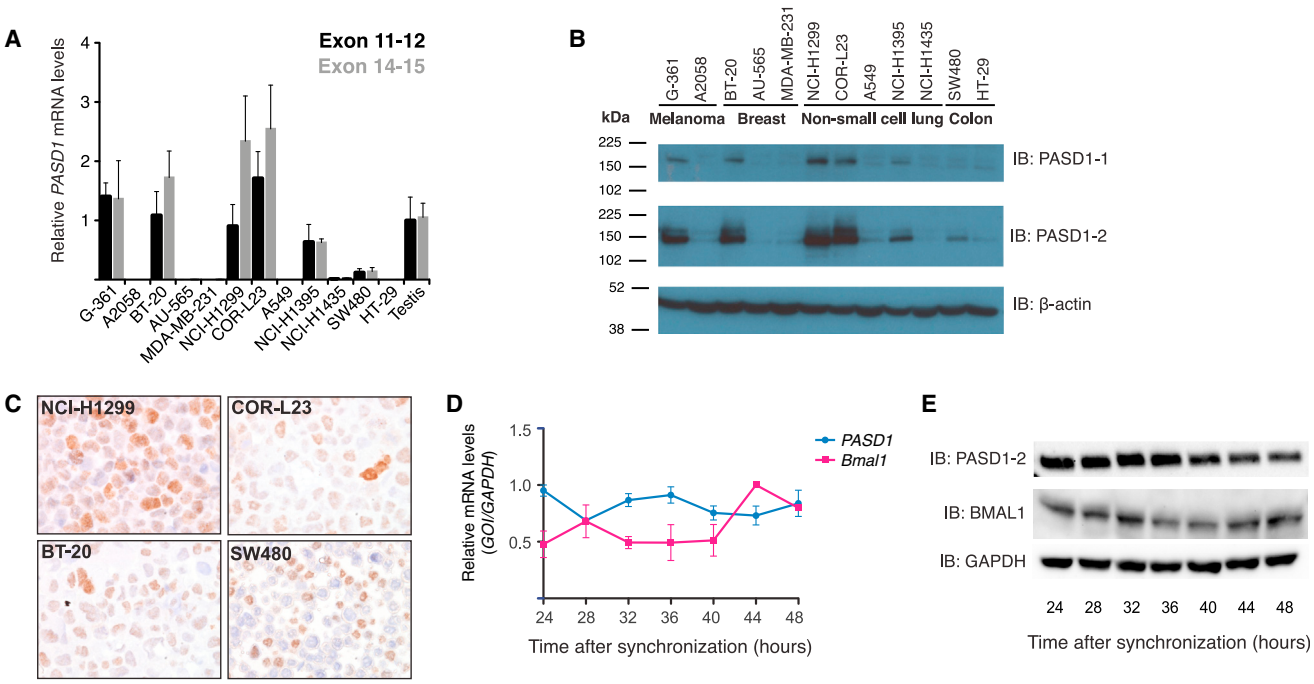

Figure 5. *PASD1* mRNA and Protein Are Expressed in a Diverse Array of Human Cancers

(A) Examination of *PASD1* transcripts in a panel of cancer cell lines by RT-qPCR. Exons 11 to 12 TaqMan probe (Hs01098424_m1) recognizes both splice isoforms, while exons 14 to 15 (Hs00542871_m1) TaqMan probe recognizes only the long isoform. *PASD1* expression was normalized to TBP (TATA box binding protein), 18S RNA and HPRT1 (hypoxanthine phosphoribosyltransferase 1), and all samples are presented relative to *PASD1* expression in human testis, normalized to 1. Error bars indicate SD from n = 3 measurements.

(B) Western blot analysis of PASD1 protein expression in the same cell lines as in (A). The PASD1-1 monoclonal antibody recognizes an epitope between residues 195 and 474, common to both splice isoforms. The PASD1-2 monoclonal antibody recognizes an epitope between residues 640 and 773 that is specific to the longer isoform (Cooper et al., 2006).

(C) Immunohistochemistry of PASD1 positive cancer cell lines. Hematoxylin and eosin staining (blue), nuclei; PASD1 staining (brown).

(D) RT-qPCR of *PASD1* and *Bmal1* in NCI-H1299 cells after circadian synchronization with 100 nM dexamethasone. Relative mRNA values are normalized to *GAPDH* and error bars represent the mean ± SEM of two independent experiments.

(E) Western blot of PASD1 and BMAL1 protein expression in circadian synchronized NCI-H1299 cells. Data are representative of two independent experiments.

expressed in human cancer cells (Figure 5A) (Cooper et al., 2006). Among cancer cell lines with the highest *PASD1* mRNA expression, we found that G-361 melanoma, NCI-H1299 non-small-cell lung carcinoma, COR-L23 large cell lung carcinoma, and the BT-20 breast cancer line had *PASD1* transcript levels comparable with human testis (Figure 5A). Relative levels of PASD1 protein correlated with differences between mRNA transcripts when analyzed by western blotting, and expression of the longer isoform was confirmed by use of isoform-specific antibodies (Figure 5B) (Cooper et al., 2006). Immunohistochemical analysis of PASD1 expression in several cancer cell lines revealed cell-to-cell heterogeneity in nuclear PASD1 expression, particularly within SW480 colon cancer cells (Figure 5C). Heterogeneous expression of cancer biomarkers is often seen in tumors and can drastically affect the efficacy of cancer therapeutics (Marusyk et al., 2012). Moreover, in the context of circadian regulation, heterogeneous expression of PASD1 could lead to differences in period among individual cells that would serve to desynchronize cell-autonomous molecular oscillators to diminish overall clock function in the tumor microenvironment.

Other repressors of CLOCK:BMAL1 are transcriptionally regulated by the clock, giving rise to a circadian peak in mRNA abundance (Albrecht et al., 1997; Anafi et al., 2014; Annayev et al., 2014; Honma et al., 2002; Miyamoto and Sancar, 1999; Shearman et al., 1997; Zhao et al., 2007). We examined *PASD1* and *Bmal1* mRNA and protein expression over a circadian period in NCI-H1299 cells after synchronization of cellular clocks by dexamethasone. We found that expression of *Bmal1* mRNA was rhythmic on the circadian timescale, but exhibited low amplitude in its oscillation (ANOVA, p = 0.05) (Figure 5D). *PASD1* mRNA expression was antiphasic to *Bmal1* with an even lower amplitude of oscillation that did not reach criteria for significance (ANOVA, p = 0.12). Protein levels of BMAL1 followed the same trend, with cyclical yet low-amplitude circadian rhythms, while PASD1 levels did not appear to cycle after synchronization (Figure 5E). Taken together, these data suggest that PASD1 may be a CLOCK:BMAL1 target; however, we were unable to detect a circadian oscillation of PASD1 mRNA or protein levels in NCI-H1299 cells.

Downregulation of PASD1 Improves Amplitude of Cycling in Human Cancer Cells

To assess the effect of endogenous PASD1 expression on circadian rhythms in human cancer cells, we chose to study

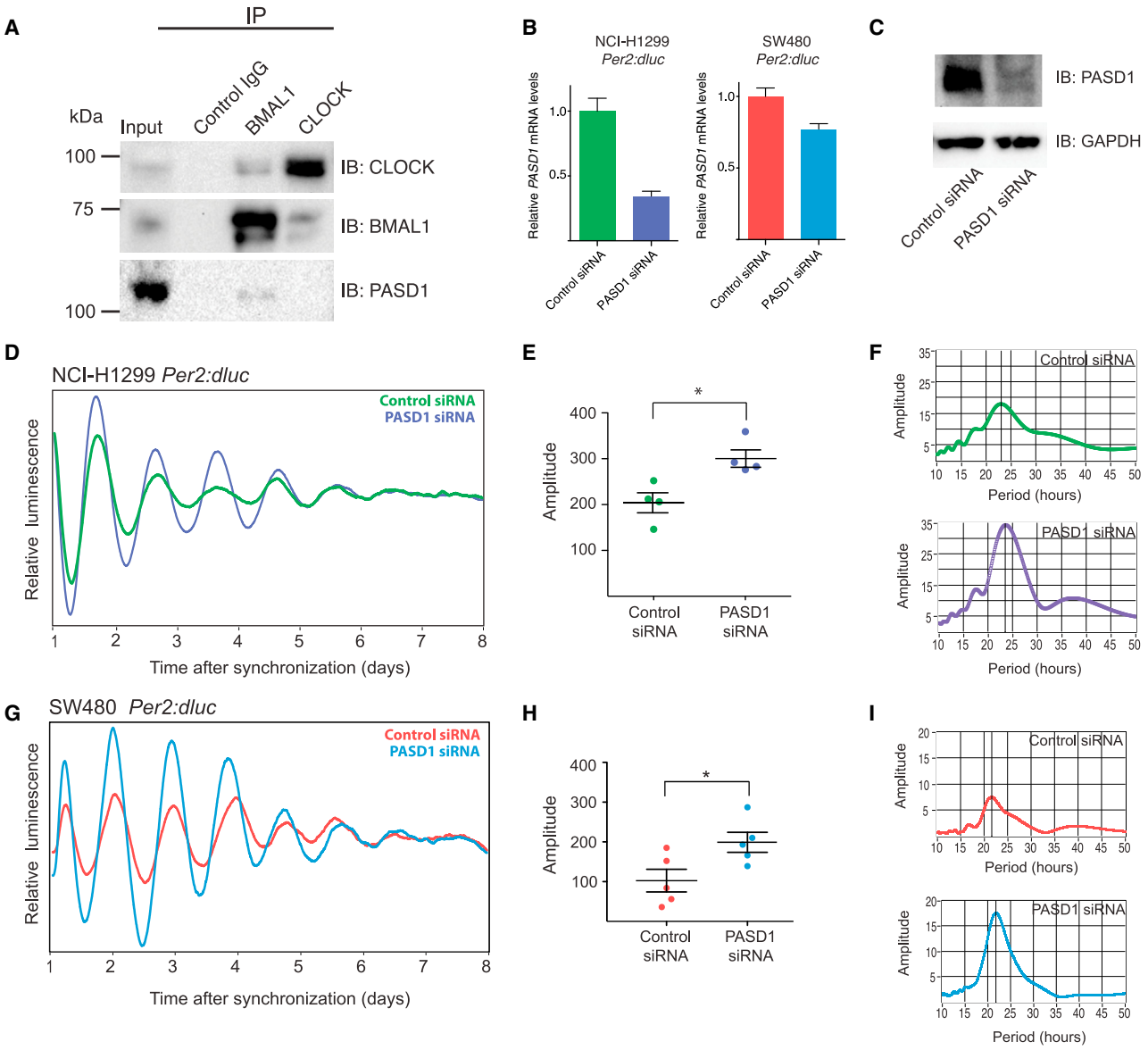

Figure 6. Reducing Expression of PASD1 in Cancer Cells Increases Robustness of Circadian Rhythms

(A) Co-immunoprecipitation of endogenous CLOCK, BMAL1, and PASD1 from NCI-H1299 nuclear extract.

(B) Reduction of *PASD1* mRNA in NCI-H1299 *Per2:dluc* (n = 3) and SW480 *Per2:dluc* (n = 4) cells after siRNA by RT-qPCR (mean ± SEM).

(C) Knockdown of PASD1 protein in NCI-H1299 *Per2:dluc* cells with siRNA. Because of the lower level of heterogeneous expression of PASD1 in SW480 cells, protein levels were at the limit of detection by western blot using our polyclonal rPASD1 antibody; therefore, knockdown was assessed only using RT-qPCR.

(D) Representative bioluminescence records from NCI-H1299 *Per2:dluc* lung cancer cells transfected with control scramble or *PASD1* siRNA (n = 4).

(E) Mean amplitude values from independent experiments. Data are represented as mean ± SEM (n = 4). Significance was assessed by Student's t test, *$p < 0.05$.

(F) FFT analysis spectrum of cycling traces shown in (D).

(G–I) Same as in (D) to (F) for SW480 *Per2:dluc* colon cancer cells. (H) Mean ± SEM (n = 5). Student's t test, *$p < 0.05$.

See also Figure S5.

the NCI-H1299 cell line (high expression) and the SW480 cell line (lower levels with more heterogeneous expression) by stably incorporating the *Per2:dluc* reporter gene (Zhang et al., 2009). Co-immunoprecipitation experiments in NCI-H1299 *Per2:dluc* cells showed that a pool of endogenous PASD1 and BMAL1 interact (Figure 6A). Transfection of the *Per2:dluc* lines with *PASD1* small interfering RNA (siRNA) achieved knockdown of PASD1 in NCI-H1299 cells as assessed by RT-qPCR, although to a lesser degree in SW480 cells (Figure 6B). siRNA treatment of NCI-H1299 *Per2:dluc* cells reduced PASD1 protein levels (Figure 6C) and resulted in a significant increase in the amplitude of circadian cycling (Figures 6D and 6E). Fast Fourier transform (FFT) power spectra of cycling data from NCI-H1299 *Per2:dluc* cells also demonstrated that knockdown of PASD1 improved

amplitude (Figure 6F). This waveform analysis converts time domain cycling data into the frequency domain, illustrating both the period of the oscillation and its amplitude, demonstrated by the height of the strongest spectral peak that defines the circadian period. The amplitude of circadian cycling was also significantly improved upon PASD1 knockdown in SW480 *Per2:dluc* cells (Figures 6G–6I). We detected a modest but non-significant trend toward a longer period in both lines with PASD1 knockdown (Figure S5). The marked improvement of cycling amplitude in two distinct cancer cell lines upon knockdown of PASD1 demonstrates that it can suppress circadian clock function when upregulated in human cancer.

DISCUSSION

Our findings establish that PASD1 is the bHLH-PAS paralog repressor for the circadian transcription factor CLOCK:BMAL1. As such, PASD1 fulfills a role analogous to the aryl hydrocarbon receptor repressor (AhRR) (Mimura et al., 1999), inhibitory PAS protein (IPAS) (Makino et al., 2001), and neuronal PAS domain protein 1 (NPAS1) (Teh et al., 2006), each dedicated to repression of a specific bHLH-PAS signaling pathway. Several bHLH-PAS paralog repressors require their homologous PAS domains to interfere with the function of cognate transcription factors (Makino et al., 2001; Mimura et al., 1999), while others, such as NPAS1 and SIM2, possess homologous PAS domains but use repressive domains in their C termini (Moffett and Pelletier, 2000; Moffett et al., 1997; Teh et al., 2006). We discovered PASD1 by searching for PAS domain-containing homologs to CLOCK and BMAL1 in humans. However, our studies addressing the biochemical mechanism of PASD1 regulation highlighted an essential role for the C-terminal CC1 domain that bears homology to the essential regulatory region encoded by CLOCK exon 19. The Id protein family also shares structural homology with CLOCK and BMAL1 in the helix-loop-helix DNA-binding domain that it uses to repress the complex (Duffield et al., 2009; Ward et al., 2010). However, by targeting a prevalent DNA-binding motif, these proteins also repress many other transcriptional networks. Because PASD1 invokes sequence similarity with CLOCK to regulate CLOCK:BMAL1 activity, it appears to be more specific for the circadian pathway. We showed that PASD1 does not repress CLOCK:BMAL1 activity like cryptochromes, which sequester the BMAL1 transcriptional activation domain from coactivators (Xu et al., 2015). Instead, PASD1 requires the activating potential of CLOCK exon 19 to repress transcriptional activation by CLOCK:BMAL1. Collectively, these data suggest that PASD1 uses molecular mimicry of CLOCK exon 19 to interfere with CLOCK:BMAL1 function.

CLOCK exon 19 is essential for CLOCK:BMAL1 function and its deletion generates a dominant-negative $Clock^{\Delta 19}$ mutant that suppresses circadian rhythms (Gekakis et al., 1998; King et al., 1997). The 51 amino acids encoded by CLOCK exon 19 are needed to interact with the coactivator histone methyltransferase MLL1 (Katada and Sassone-Corsi, 2010) and a vertebrate-specific repressor, CLOCK-interacting protein circadian (CIPC) (Zhao et al., 2007). Even though MLL1 interacts with both CLOCK and BMAL1 by co-immunoprecipitation, it requires CLOCK exon 19 to coordinate rhythmic changes in histone H3 lysine4 trimethylation (Katada and Sassone-Corsi, 2010). Unlike MLL1 and CIPC, we did not detect interaction of PASD1 with CLOCK; instead, our data show that PASD1 requires its CC1 domain to interfere with CLOCK:BMAL1 function that is mediated by exon 19. The reciprocal relationship between PASD1 CC1 and CLOCK exon 19 is further supported by similarities between PASD1 overexpression in 3T3 fibroblasts and heterozygous expression of the dominant-negative $Clock^{\Delta 19}$ mutant, both of which exhibit decreased amplitude, long period, and rapid damping (Vitaterna et al., 2006). However, the exact mechanism by which PASD1 impinges on transcriptional activation by CLOCK:BMAL1 remains to be determined.

The limited distribution of PASD1 across tissues is analogous to other bHLH-PAS repressors that are expressed selectively to control developmental or tissue-specific programs of transcriptional activation (Fan et al., 1996; Makino et al., 2001; Michael and Partch, 2013; Yamamoto et al., 2004). One powerful example of this is inhibition of the hypoxia inducible factor (HIF) (HIF-1α:ARNT) in the hypoxic cornea by its paralog repressor IPAS, which prevents neovascularization in the cornea that would interfere with vision (Makino et al., 2001). By virtue of its limited tissue distribution, PASD1 is poised to suppress circadian rhythms in the germline and, as a consequence of its demethylation and upregulation, in somatic cancers (Cooper et al., 2006; Whitehurst, 2014). Notably, mouse and hamster testis do not exhibit molecular circadian rhythms (Alvarez and Sehgal, 2005; Miyamoto and Sancar, 1999; Morse et al., 2003). It has yet to be demonstrated that testes from other mammals, including humans, do not have circadian rhythms; however, on the basis of the data presented here, we speculate that high levels of PASD1 in human testis could lead to suppression of circadian rhythms in the germline (Cooper et al., 2006). Connections between the lack of circadian cycling in undifferentiated embryonic stem cells and the germline are just coming to light (Paulose et al., 2012; Umemura et al., 2014; Yagita et al., 2010), making PASD1 an interesting link that could be explored further.

To date, cancer/testis antigens have been explored largely as targets for cancer immunotherapy (Ait-Tahar et al., 2009; Joseph-Pietras et al., 2010; Whitehurst, 2014). It is still unclear whether they simply serve as cancer biomarkers or whether their upregulation in somatic cancer has consequences for tumor progression by promoting return to a germ-like state (Simpson et al., 2005). Recent studies show that some cancer/testis antigens possess activities consistent with the latter hypothesis, from promoting destabilization of tumor suppressors to regulating genomic stability (Cappell et al., 2012; Doyle et al., 2010). Here we describe a role for a cancer/testis antigen in suppression of the circadian clock, showing that PASD1 can attenuate clock function even when heterogeneously expressed in cancer cells. Circadian disruption has been connected to increased incidence of diabetes, cardiovascular disease, and cancer (Filipski and Lévi, 2009; Jeyaraj et al., 2012; Marcheva et al., 2010), but there is a growing appreciation for reciprocal regulation of circadian rhythms by disease or altered metabolic states. In particular, consumption of a high-fat diet alters the metabolic state to suppress CLOCK:BMAL1-driven transcriptional activation and dampen circadian amplitudes, allowing the rewiring of vast

transcriptional programs (Eckel-Mahan et al., 2013; Hatori et al., 2012). These studies demonstrate the importance of maintaining robust circadian amplitudes to promote proper temporal regulation of physiology. Our discovery of PASD1 as a circadian bHLH-PAS paralog repressor that is only expressed in somatic tissues after oncogenic transformation suggests that it may represent a molecular link from oncogenesis to circadian disruption.

EXPERIMENTAL PROCEDURES

Immunofluorescence

Cells were fixed with 4% paraformaldehyde for 10 min, then permeabilized and blocked in PBS containing 1% horse serum and 0.05% Triton X-100 for 15 min. Primary incubation was carried out for 1 hr at room temperature in blocking solution with chicken anti-GFP (1:1,500; Aves Labs) or mouse anti-MYC (1:1,000; Abcam). Cells were washed three times with PBS, then incubated with secondary Alexa Fluor conjugated antibodies (1:2,000; Molecular Probes) and DAPI (Life Technologies) for 30 min. Slides were mounted in Fluoromount-G (Southern Biotech) and analyzed on a Keyence BZ-9000 fluorescence microscope.

Antibodies

Polyclonal antibodies were generated against human PASD1 (rPASD1) (epitope: DQMRSAEQTRLMPAEQRDS, residues 751–770) and human BMAL1 (Rey et al., 2011) (epitope: LEADAGLGGPVDFSDLPWPL, residues 607–626) by immunization of KLH-conjugated peptides in rabbits using standard protocols (Pierce Biotechnology). Serum was affinity purified using the SulfoLink Immobiliation Kit using the manufacturer's instructions (Thermo) after conjugation of the antigenic peptide to the immobile phase. Purified antibodies were dialyzed into 0.15 M glycine, 50 mM Tris-HCl (pH 7.0) with 50% glycerol and aliquoted for storage at −80°C. Hybridoma supernatants containing anti-PASD1 monoclonal antibodies (PASD1-1 and PASD1-2) were as previously described (Cooper et al., 2006).

SUPPLEMENTAL INFORMATION

Supplemental Information includes Supplemental Experimental Procedures, five figures, and two tables and can be found with this article online at http://dx.doi.org/10.1016/j.molcel.2015.03.031.

ACKNOWLEDGMENTS

We appreciate comments from A. Sancar, A.C. Liu, and L. Hinck on the manuscript. This work was supported by grants from the University of California Cancer Research Coordinating Committee and National Institutes of Health grant R01 GM107069 (to C.L.P), National Institutes of Health Ruth Kirschstein Fellowship F31 CA189660 and a Paul & Anne Irwin Cancer Research Award (to A.K.M.), and Cancer Research UK Programme grant A10702 (to A.H.B.).

Received: November 23, 2014
Revised: February 13, 2015
Accepted: March 25, 2015
Published: April 30, 2015

REFERENCES

Ait-Tahar, K., Liggins, A.P., Collins, G.P., Campbell, A., Barnardo, M., Lawrie, C., Moir, D., Hatton, C., Banham, A.H., and Pulford, K. (2009). Cytolytic T-cell response to the PASD1 cancer testis antigen in patients with diffuse large B-cell lymphoma. Br. J. Haematol. *146*, 396–407.

Albrecht, U., Sun, Z.S., Eichele, G., and Lee, C.C. (1997). A differential response of two putative mammalian circadian regulators, mper1 and mper2, to light. Cell *91*, 1055–1064.

Alvarez, J.D., and Sehgal, A. (2005). The thymus is similar to the testis in its pattern of circadian clock gene expression. J. Biol. Rhythms *20*, 111–121.

Anafi, R.C., Lee, Y., Sato, T.K., Venkataraman, A., Ramanathan, C., Kavakli, I.H., Hughes, M.E., Baggs, J.E., Growe, J., Liu, A.C., et al. (2014). Machine learning helps identify CHRONO as a circadian clock component. PLoS Biol. *12*, e1001840.

Annayev, Y., Adar, S., Chiou, Y.-Y., Lieb, J.D., Sancar, A., and Ye, R. (2014). Gene model 129 (Gm129) encodes a novel transcriptional repressor that modulates circadian gene expression. J. Biol. Chem. *289*, 5013–5024.

Cappell, K.M., Sinnott, R., Taus, P., Maxfield, K., Scarbrough, M., and Whitehurst, A.W. (2012). Multiple cancer testis antigens function to support tumor cell mitotic fidelity. Mol. Cell. Biol. *32*, 4131–4140.

Cooper, C.D.O., Liggins, A.P., Ait-Tahar, K., Roncador, G., Banham, A.H., and Pulford, K. (2006). PASD1, a DLBCL-associated cancer testis antigen and candidate for lymphoma immunotherapy. Leukemia *20*, 2172–2174.

Crews, S.T. (1998). Control of cell lineage-specific development and transcription by bHLH-PAS proteins. Genes Dev. *12*, 607–620.

Czarna, A., Breitkreuz, H., Mahrenholz, C.C., Arens, J., Strauss, H.M., and Wolf, E. (2011). Quantitative analyses of cryptochrome-mBMAL1 interactions: mechanistic insights into the transcriptional regulation of the mammalian circadian clock. J. Biol. Chem. *286*, 22414–22425.

Dioum, E.M., Chen, R., Alexander, M.S., Zhang, Q., Hogg, R.T., Gerard, R.D., and Garcia, J.A. (2009). Regulation of hypoxia-inducible factor 2alpha signaling by the stress-responsive deacetylase sirtuin 1. Science *324*, 1289–1293.

Djureinovic, D., Fagerberg, L., Hallström, B., Danielsson, A., Lindskog, C., Uhlén, M., and Pontén, F. (2014). The human testis-specific proteome defined by transcriptomics and antibody-based profiling. Mol. Hum. Reprod. *20*, 476–488.

Doi, M., Hirayama, J., and Sassone-Corsi, P. (2006). Circadian regulator CLOCK is a histone acetyltransferase. Cell *125*, 497–508.

Doyle, J.M., Gao, J., Wang, J., Yang, M., and Potts, P.R. (2010). MAGE-RING protein complexes comprise a family of E3 ubiquitin ligases. Mol. Cell *39*, 963–974.

Duffield, G.E., Watson, N.P., Mantani, A., Peirson, S.N., Robles-Murguia, M., Loros, J.J., Israel, M.A., and Dunlap, J.C. (2009). A role for Id2 in regulating photic entrainment of the mammalian circadian system. Curr. Biol. *19*, 297–304.

Eckel-Mahan, K.L., Patel, V.R., de Mateo, S., Orozco-Solis, R., Ceglia, N.J., Sahar, S., Dilag-Penilla, S.A., Dyar, K.A., Baldi, P., and Sassone-Corsi, P. (2013). Reprogramming of the circadian clock by nutritional challenge. Cell *155*, 1464–1478.

Ema, M., Morita, M., Ikawa, S., Tanaka, M., Matsuda, Y., Gotoh, O., Saijoh, Y., Fujii, H., Hamada, H., Kikuchi, Y., and Fujii-Kuriyama, Y. (1996). Two new members of the murine Sim gene family are transcriptional repressors and show different expression patterns during mouse embryogenesis. Mol. Cell. Biol. *16*, 5865–5875.

Evans, B.R., Karchner, S.I., Allan, L.L., Pollenz, R.S., Tanguay, R.L., Jenny, M.J., Sherr, D.H., and Hahn, M.E. (2008). Repression of aryl hydrocarbon receptor (AHR) signaling by AHR repressor: role of DNA binding and competition for AHR nuclear translocator. Mol. Pharmacol. *73*, 387–398.

Fan, C.M., Kuwana, E., Bulfone, A., Fletcher, C.F., Copeland, N.G., Jenkins, N.A., Crews, S., Martinez, S., Puelles, L., Rubenstein, J.L., and Tessier-Lavigne, M. (1996). Expression patterns of two murine homologs of Drosophila single-minded suggest possible roles in embryonic patterning and in the pathogenesis of Down syndrome. Mol. Cell. Neurosci. *7*, 1–16.

Filipski, E., and Lévi, F. (2009). Circadian disruption in experimental cancer processes. Integr. Cancer Ther. *8*, 298–302.

Freedman, S.J., Sun, Z.-Y.J., Poy, F., Kung, A.L., Livingston, D.M., Wagner, G., and Eck, M.J. (2002). Structural basis for recruitment of CBP/p300 by hypoxia-inducible factor-1 alpha. Proc. Natl. Acad. Sci. U S A *99*, 5367–5372.

Gekakis, N., Staknis, D., Nguyen, H.B., Davis, F.C., Wilsbacher, L.D., King, D.P., Takahashi, J.S., and Weitz, C.J. (1998). Role of the CLOCK protein in the mammalian circadian mechanism. Science *280*, 1564–1569.

Gu, Y.Z., Moran, S.M., Hogenesch, J.B., Wartman, L., and Bradfield, C.A. (1998). Molecular characterization and chromosomal localization of a third alpha-class hypoxia inducible factor subunit, HIF3alpha. Gene Expr. *7*, 205–213.

Gustafson, C.L., and Partch, C.L. (2014). Emerging models for the molecular basis of mammalian circadian timing. Biochemistry *54*, 134–149.

Hatori, M., Vollmers, C., Zarrinpar, A., DiTacchio, L., Bushong, E.A., Gill, S., Leblanc, M., Chaix, A., Joens, M., Fitzpatrick, J.A.J., et al. (2012). Time-restricted feeding without reducing caloric intake prevents metabolic diseases in mice fed a high-fat diet. Cell Metab. *15*, 848–860.

Hirota, T., Lewis, W.G., Liu, A.C., Lee, J.W., Schultz, P.G., and Kay, S.A. (2008). A chemical biology approach reveals period shortening of the mammalian circadian clock by specific inhibition of GSK-3β. Proc. Natl. Acad. Sci. U S A *105*, 20746–20751.

Honma, S., Kawamoto, T., Takagi, Y., Fujimoto, K., Sato, F., Noshiro, M., Kato, Y., and Honma, K. (2002). Dec1 and Dec2 are regulators of the mammalian molecular clock. Nature *419*, 841–844.

Huang, N., Chelliah, Y., Shan, Y., Taylor, C.A., Yoo, S.-H., Partch, C., Green, C.B., Zhang, H., and Takahashi, J.S. (2012). Crystal structure of the heterodimeric CLOCK:BMAL1 transcriptional activator complex. Science *337*, 189–194.

Izumo, M., Sato, T.R., Straume, M., and Johnson, C.H. (2006). Quantitative analyses of circadian gene expression in mammalian cell cultures. PLoS Comput. Biol. *2*, e136.

Jeyaraj, D., Haldar, S.M., Wan, X., McCauley, M.D., Ripperger, J.A., Hu, K., Lu, Y., Eapen, B.L., Sharma, N., Ficker, E., et al. (2012). Circadian rhythms govern cardiac repolarization and arrhythmogenesis. Nature *483*, 96–99.

Joseph-Pietras, D., Gao, Y., Zojer, N., Ait-Tahar, K., Banham, A.H., Pulford, K., Rice, J., Savelyeva, N., and Sahota, S.S. (2010). DNA vaccines to target the cancer testis antigen PASD1 in human multiple myeloma. Leukemia *24*, 1951–1959.

Katada, S., and Sassone-Corsi, P. (2010). The histone methyltransferase MLL1 permits the oscillation of circadian gene expression. Nat. Struct. Mol. Biol. *17*, 1414–1421.

Kim, R., Kulkarni, P., and Hannenhalli, S. (2013). Derepression of Cancer/testis antigens in cancer is associated with distinct patterns of DNA hypomethylation. BMC Cancer *13*, 144.

King, D.P., Zhao, Y., Sangoram, A.M., Wilsbacher, L.D., Tanaka, M., Antoch, M.P., Steeves, T.D., Vitaterna, M.H., Kornhauser, J.M., Lowrey, P.L., et al. (1997). Positional cloning of the mouse circadian clock gene. Cell *89*, 641–653.

Kiyohara, Y.B., Tagao, S., Tamanini, F., Morita, A., Sugisawa, Y., Yasuda, M., Yamanaka, I., Ueda, H.R., van der Horst, G.T.J., Kondo, T., and Yagita, K. (2006). The BMAL1 C terminus regulates the circadian transcription feedback loop. Proc. Natl. Acad. Sci. U S A *103*, 10074–10079.

Kobayashi, A., Numayama-Tsuruta, K., Sogawa, K., and Fujii-Kuriyama, Y. (1997). CBP/p300 functions as a possible transcriptional coactivator of Ah receptor nuclear translocator (Arnt). J. Biochem. *122*, 703–710.

Koike, N., Yoo, S.-H., Huang, H.-C., Kumar, V., Lee, C., Kim, T.-K., and Takahashi, J.S. (2012). Transcriptional architecture and chromatin landscape of the core circadian clock in mammals. Science *338*, 349–354.

Kondratov, R.V., Chernov, M.V., Kondratova, A.A., Gorbacheva, V.Y., Gudkov, A.V., and Antoch, M.P. (2003). BMAL1-dependent circadian oscillation of nuclear CLOCK: posttranslational events induced by dimerization of transcriptional activators of the mammalian clock system. Genes Dev. *17*, 1921–1932.

Kondratov, R.V., Kondratova, A.A., Gorbacheva, V.Y., Vykhovanets, O.V., and Antoch, M.P. (2006). Early aging and age-related pathologies in mice deficient in BMAL1, the core componentof the circadian clock. Genes Dev. *20*, 1868–1873.

Kwon, I., Lee, J., Chang, S.H., Jung, N.C., Lee, B.J., Son, G.H., Kim, K., and Lee, K.H. (2006). BMAL1 shuttling controls transactivation and degradation of the CLOCK/BMAL1 heterodimer. Mol. Cell. Biol. *26*, 7318–7330.

Lee, C., Etchegaray, J.P., Cagampang, F.R., Loudon, A.S., and Reppert, S.M. (2001). Posttranslational mechanisms regulate the mammalian circadian clock. Cell *107*, 855–867.

Letunic, I., Doerks, T., and Bork, P. (2015). SMART: recent updates, new developments and status in 2015. Nucleic Acids Res. *43*, D257–D260.

Liggins, A.P., Brown, P.J., Asker, K., Pulford, K., and Banham, A.H. (2004). A novel diffuse large B-cell lymphoma-associated cancer testis antigen encoding a PAS domain protein. Br. J. Cancer *91*, 141–149.

Liggins, A.P., Lim, S.H., Soilleux, E.J., Pulford, K., and Banham, A.H. (2010). A panel of cancer-testis genes exhibiting broad-spectrum expression in haematological malignancies. Cancer Immun. a J. Acad. Cancer Immunol. *10*, 8.

Makino, Y., Cao, R., Svensson, K., Bertilsson, G., Asman, M., Tanaka, H., Cao, Y., Berkenstam, A., and Poellinger, L. (2001). Inhibitory PAS domain protein is a negative regulator of hypoxia-inducible gene expression. Nature *414*, 550–554.

Marcheva, B., Ramsey, K.M., Buhr, E.D., Kobayashi, Y., Su, H., Ko, C.H., Ivanova, G., Omura, C., Mo, S., Vitaterna, M.H., et al. (2010). Disruption of the clock components CLOCK and BMAL1 leads to hypoinsulinaemia and diabetes. Nature *466*, 627–631.

Marusyk, A., Almendro, V., and Polyak, K. (2012). Intra-tumour heterogeneity: a looking glass for cancer? Nat. Rev. Cancer *12*, 323–334.

Michael, A.K., and Partch, C.L. (2013). bHLH-PAS proteins: functional specification through modular domain architecture. OA Biochem. *1*, 16.

Mimura, J., Ema, M., Sogawa, K., and Fujii-Kuriyama, Y. (1999). Identification of a novel mechanism of regulation of Ah (dioxin) receptor function. Genes Dev. *13*, 20–25.

Miyamoto, Y., and Sancar, A. (1999). Circadian regulation of cryptochrome genes in the mouse. Brain Res. Mol. Brain Res. *71*, 238–243.

Moffett, P., and Pelletier, J. (2000). Different transcriptional properties of mSim-1 and mSim-2. FEBS Lett. *466*, 80–86.

Moffett, P., Reece, M., and Pelletier, J. (1997). The murine Sim-2 gene product inhibits transcription by active repression and functional interference. Mol. Cell. Biol. *17*, 4933–4947.

Morse, D., Cermakian, N., Brancorsini, S., Parvinen, M., and Sassone-Corsi, P. (2003). No circadian rhythms in testis: Period1 expression is clock independent and developmentally regulated in the mouse. Mol. Endocrinol. *17*, 141–151.

Mueller, J.L., Skaletsky, H., Brown, L.G., Zaghlul, S., Rock, S., Graves, T., Auger, K., Warren, W.C., Wilson, R.K., and Page, D.C. (2013). Independent specialization of the human and mouse X chromosomes for the male germ line. Nat. Genet. *45*, 1083–1087.

Nagoshi, E., Saini, C., Bauer, C., Laroche, T., Naef, F., and Schibler, U. (2004). Circadian gene expression in individual fibroblasts: cell-autonomous and self-sustained oscillators pass time to daughter cells. Cell *119*, 693–705.

Padeken, J., and Heun, P. (2014). Nucleolus and nuclear periphery: velcro for heterochromatin. Curr. Opin. Cell Biol. *28*, 54–60.

Panda, S., Antoch, M.P., Miller, B.H., Su, A.I., Schook, A.B., Straume, M., Schultz, P.G., Kay, S.A., Takahashi, J.S., and Hogenesch, J.B. (2002). Coordinated transcription of key pathways in the mouse by the circadian clock. Cell *109*, 307–320.

Paulose, J.K., Rucker, E.B., 3rd, and Cassone, V.M. (2012). Toward the beginning of time: circadian rhythms in metabolism precede rhythms in clock gene expression in mouse embryonic stem cells. PLoS ONE *7*, e49555.

Rey, G., Cesbron, F., Rougemont, J., Reinke, H., Brunner, M., and Naef, F. (2011). Genome-wide and phase-specific DNA-binding rhythms of BMAL1 control circadian output functions in mouse liver. PLoS Biol. *9*, e1000595.

Sahar, S., and Sassone-Corsi, P. (2009). Metabolism and cancer: the circadian clock connection. Nat. Rev. Cancer *9*, 886–896.

Scheuermann, T.H., Tomchick, D.R., Machius, M., Guo, Y., Bruick, R.K., and Gardner, K.H. (2009). Artificial ligand binding within the HIF2alpha PAS-B domain of the HIF2 transcription factor. Proc. Natl. Acad. Sci. U S A *106*, 450–455.

Schultz, J., Milpetz, F., Bork, P., and Ponting, C.P. (1998). SMART, a simple modular architecture research tool: identification of signaling domains. Proc. Natl. Acad. Sci. U S A *95*, 5857–5864.

Shearman, L.P., Zylka, M.J., Weaver, D.R., Kolakowski, L.F., Jr., and Reppert, S.M. (1997). Two period homologs: circadian expression and photic regulation in the suprachiasmatic nuclei. Neuron *19*, 1261–1269.

Simpson, A.J.G., Caballero, O.L., Jungbluth, A., Chen, Y.-T., and Old, L.J. (2005). Cancer/testis antigens, gametogenesis and cancer. Nat. Rev. Cancer *5*, 615–625.

Storch, K.-F., Lipan, O., Leykin, I., Viswanathan, N., Davis, F.C., Wong, W.H., and Weitz, C.J. (2002). Extensive and divergent circadian gene expression in liver and heart. Nature *417*, 78–83.

Takahashi, J.S., Hong, H.-K., Ko, C.H., and McDearmon, E.L. (2008). The genetics of mammalian circadian order and disorder: implications for physiology and disease. Nat. Rev. Genet. *9*, 764–775.

Takahata, S., Ozaki, T., Mimura, J., Kikuchi, Y., Sogawa, K., and Fujii-Kuriyama, Y. (2000). Transactivation mechanisms of mouse clock transcription factors, mClock and mArnt3. Genes Cells *5*, 739–747.

Teh, C.H.L., Lam, K.K.Y., Loh, C.C., Loo, J.M., Yan, T., and Lim, T.M. (2006). Neuronal PAS domain protein 1 is a transcriptional repressor and requires arylhydrocarbon nuclear translocator for its nuclear localization. J. Biol. Chem. *281*, 34617–34629.

Umemura, Y., Koike, N., Matsumoto, T., Yoo, S.-H., Chen, Z., Yasuhara, N., Takahashi, J.S., and Yagita, K. (2014). Transcriptional program of Kpna2/Importin-α2 regulates cellular differentiation-coupled circadian clock development in mammalian cells. Proc. Natl. Acad. Sci. U S A *111*, E5039–E5048.

Vitaterna, M.H., Ko, C.H., Chang, A.-M., Buhr, E.D., Fruechte, E.M., Schook, A., Antoch, M.P., Turek, F.W., and Takahashi, J.S. (2006). The mouse Clock mutation reduces circadian pacemaker amplitude and enhances efficacy of resetting stimuli and phase-response curve amplitude. Proc. Natl. Acad. Sci. U S A *103*, 9327–9332.

Vollmers, C., Panda, S., and DiTacchio, L. (2008). A high-throughput assay for siRNA-based circadian screens in human U2OS cells. PLoS ONE *3*, e3457.

Wang, Z., Wu, Y., Li, L., and Su, X.-D. (2013). Intermolecular recognition revealed by the complex structure of human CLOCK-BMAL1 basic helix-loop-helix domains with E-box DNA. Cell Res. *23*, 213–224.

Ward, S.M., Fernando, S.J., Hou, T.Y., and Duffield, G.E. (2010). The transcriptional repressor ID2 can interact with the canonical clock components CLOCK and BMAL1 and mediate inhibitory effects on mPer1 expression. J. Biol. Chem. *285*, 38987–39000.

Welsh, D.K., Yoo, S.H., Liu, A.C., Takahashi, J.S., and Kay, S.A. (2004). Bioluminescence imaging of individual fibroblasts reveals persistent, independently phased circadian rhythms of clock gene expression. Curr. Biol. *14*, 2289–2295.

Whitehurst, A.W. (2014). Cause and consequence of cancer/testis antigen activation in cancer. Annu. Rev. Pharmacol. Toxicol. *54*, 251–272.

Xu, H., Gustafson, C.L., Sammons, P.J., Khan, S.K., Parsley, N.C., Ramanathan, C., Lee, H.-W., Liu, A.C., and Partch, C.L. (2015). Cryptochrome 1 regulates the circadian clock through dynamic interactions with the BMAL1 C-terminus. Nat. Struct. Mol. Biol. Published May 11, 2015. http://dx.doi.org/10.1038/nsmb.3018.

Yagita, K., Horie, K., Koinuma, S., Nakamura, W., Yamanaka, I., Urasaki, A., Shigeyoshi, Y., Kawakami, K., Shimada, S., Takeda, J., and Uchiyama, Y. (2010). Development of the circadian oscillator during differentiation of mouse embryonic stem cells in vitro. Proc. Natl. Acad. Sci. U S A *107*, 3846–3851.

Yamamoto, J., Ihara, K., Nakayama, H., Hikino, S., Satoh, K., Kubo, N., Iida, T., Fujii, Y., and Hara, T. (2004). Characteristic expression of aryl hydrocarbon receptor repressor gene in human tissues: organ-specific distribution and variable induction patterns in mononuclear cells. Life Sci. *74*, 1039–1049.

Yoo, S.-H., Yamazaki, S., Lowrey, P.L., Shimomura, K., Ko, C.H., Buhr, E.D., Siepka, S.M., Hong, H.-K., Oh, W.J., Yoo, O.J., et al. (2004). PERIOD2::LUCIFERASE real-time reporting of circadian dynamics reveals persistent circadian oscillations in mouse peripheral tissues. Proc. Natl. Acad. Sci. U S A *101*, 5339–5346.

Zhang, E.E., Liu, A.C., Hirota, T., Miraglia, L.J., Welch, G., Pongsawakul, P.Y., Liu, X., Atwood, A., Huss, J.W., 3rd, Janes, J., et al. (2009). A genome-wide RNAi screen for modifiers of the circadian clock in human cells. Cell *139*, 199–210.

Zhang, R., Lahens, N.F., Ballance, H.I., Hughes, M.E., and Hogenesch, J.B. (2014). A circadian gene expression atlas in mammals: implications for biology and medicine. Proc. Natl. Acad. Sci. U S A *111*, 16219–16224.

Zhao, W.-N., Malinin, N., Yang, F.-C., Staknis, D., Gekakis, N., Maier, B., Reischl, S., Kramer, A., and Weitz, C.J. (2007). CIPC is a mammalian circadian clock protein without invertebrate homologues. Nat. Cell Biol. *9*, 268–275.

Molecular Cell

Supplemental Information

Cancer/Testis Antigen PASD1 Silences the Circadian Clock

Alicia K. Michael, Stacy L. Harvey, Patrick J. Sammons, Amanda P. Anderson, Hema M. Kopalle, Alison H. Banham, and Carrie L. Partch

Supplemental Data

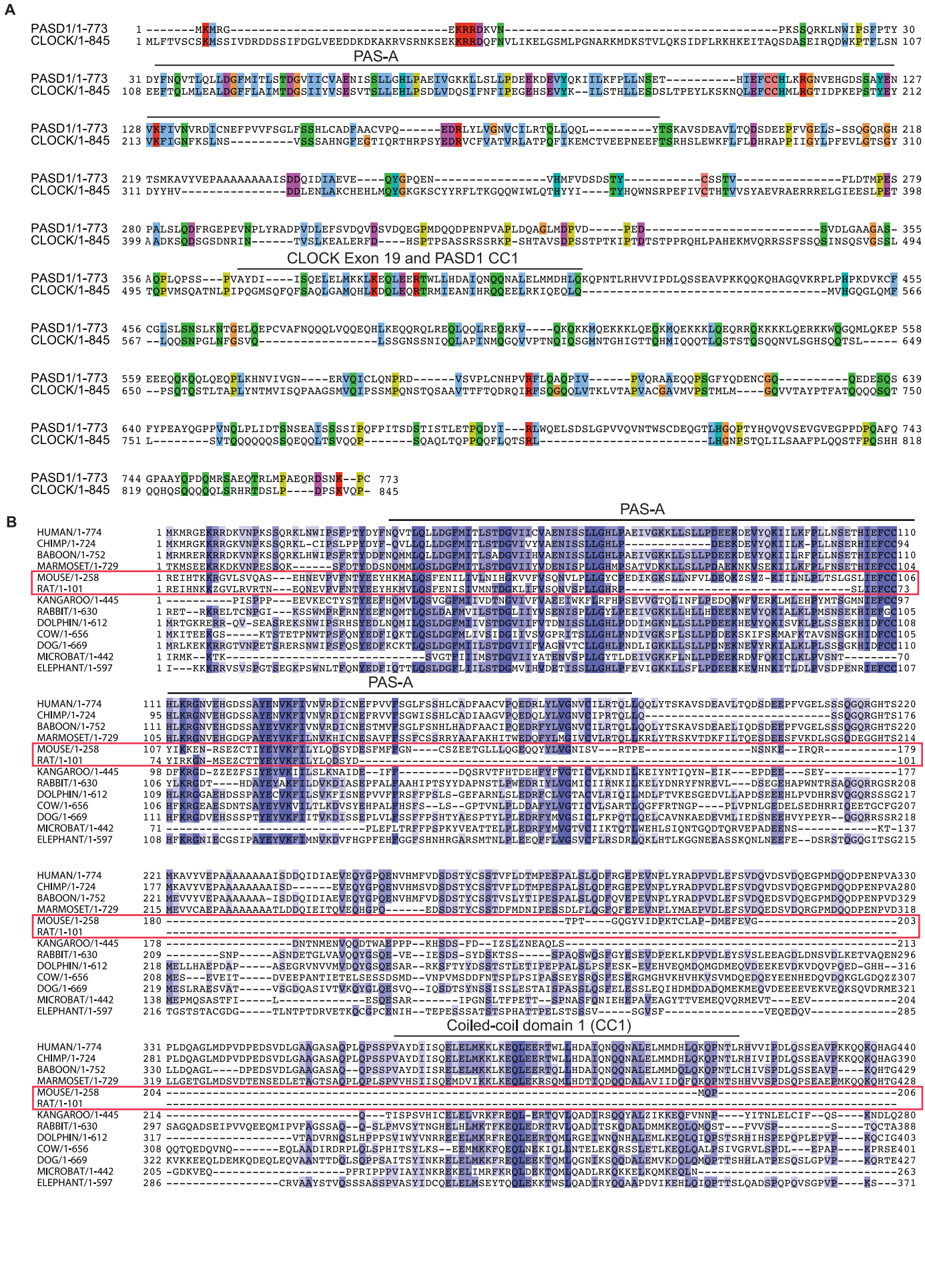

Figure S1. Human PASD1 has significant sequence homology with CLOCK and lacks a murine homolog. (related to Figure 1)

(A) Clustalx alignment of human PASD1 (NP_775764.2) aligned with human CLOCK using Multiple Alignment Fast Fourier Transform. Regions of high identity between the PAS-A domains (34%) or the Exon 19 of CLOCK and CC1 domain of PASD1 (36%) are highlighted with a thick black line.

(B) Multiple sequence alignment of PASD1 proteins across mammals were generated using the UCSC genome browser Vertebrate Multiz Alignment track and displayed using Jalview. Only residues corresponding to human PASD1 1 – 400 are shown due to space constraints. While the mouse gm1141 (accession: B9EJU1) is annotated as *PASD1* in the mouse genome (mm10), it shows very low sequence identity with the *PASD1* gene found in mammals. The predicted mouse transcript from the UCSC genome browser Vertebrate Multiz Alignment has a higher degree of identity and is shown here. The red box highlights the putative protein product of the truncated gene in mice and rats.

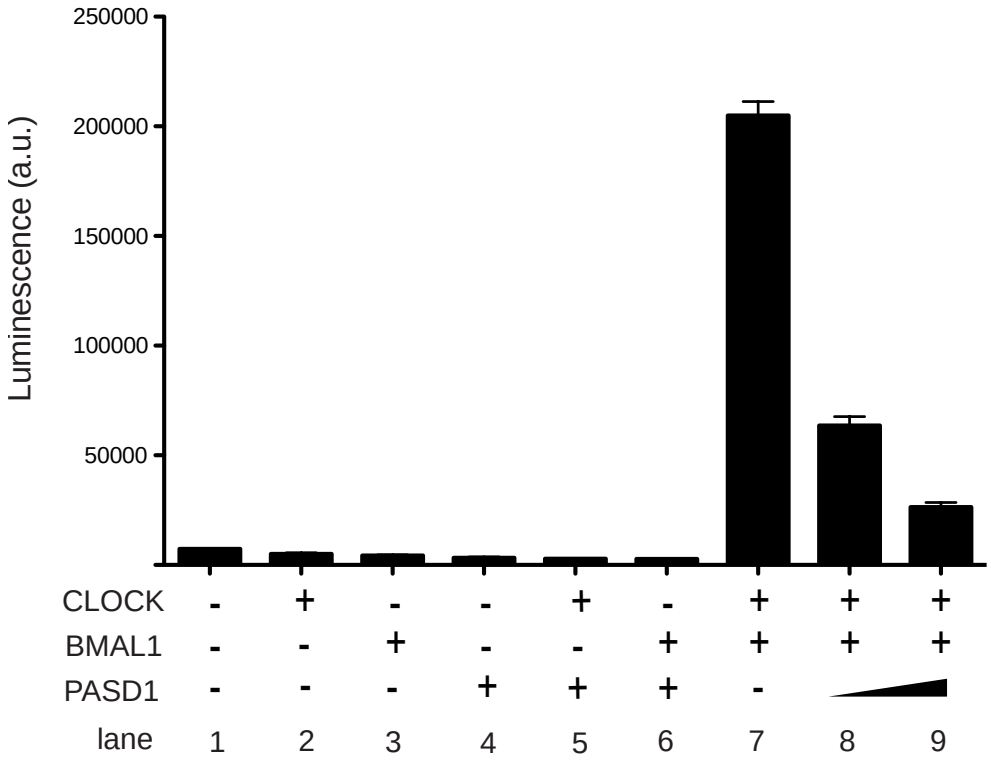

Figure S2. Co-transfection of PASD1 with CLOCK or BMAL1 does not transactivate the *Per1:luc* gene. (related to Figure 2)

HEK293T cells were transfected with the *Per1:luc* reporter gene plasmid alone (lane 1), or with CLOCK, BMAL1 or PASD1 alone as indicated (lanes 2-4). PASD1 cannot drive activation of the *Per1:luc* reporter gene in combination with either CLOCK or BMAL1 (lanes 5 and 6). Co-transfection of CLOCK and BMAL1 results in 25 - 30 fold activation over the background of the *Per1:luc* reporter gene alone (lane 7) that is repressed by PASD1 (lanes 8-9). Raw luminescence counts from a representative assay (in triplicate) are shown ± SD.

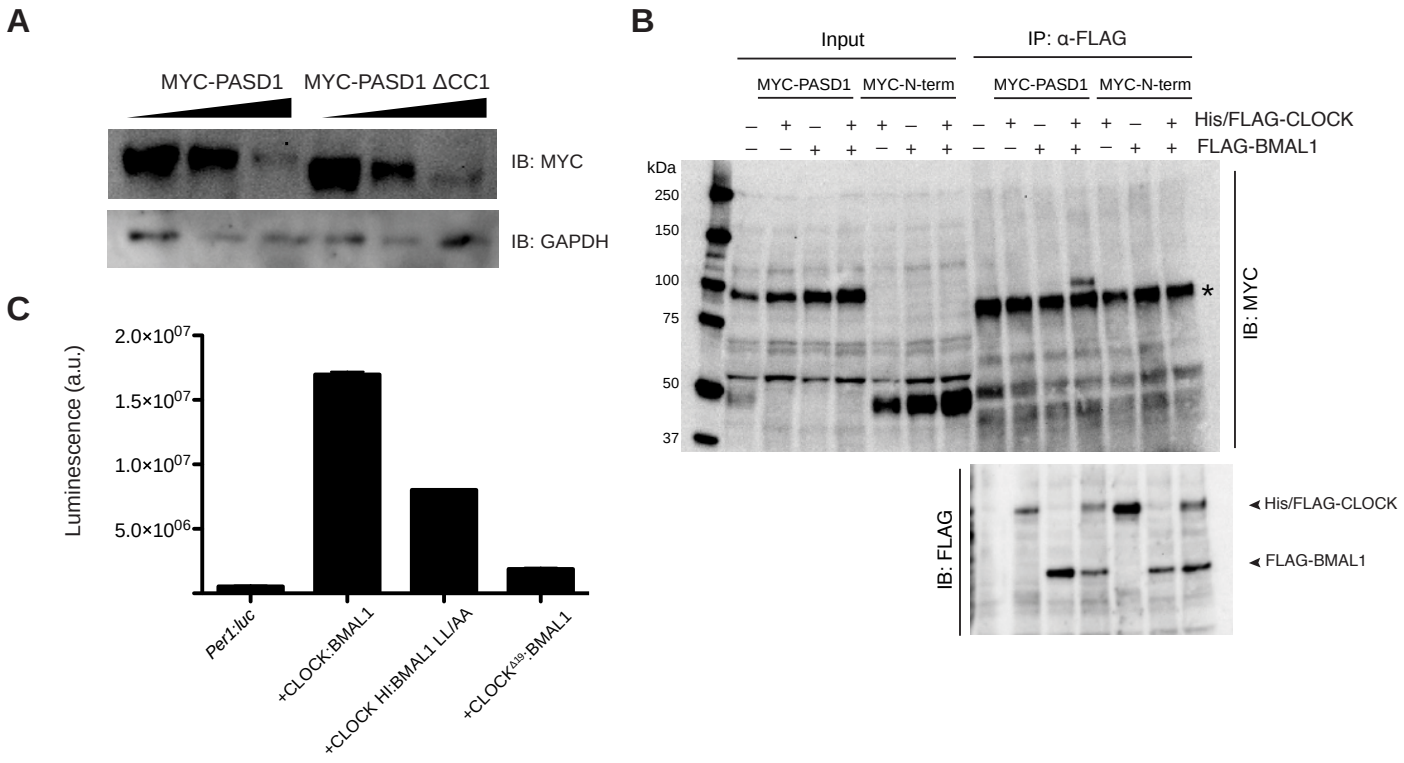

Figure S3. Characterization of PASD1 and CLOCK:BMAL1 mutants. (related to Figure 3)
(A) PASD1ΔCC1 shows similar expression levels compared to the full length protein when over-expressed. HEK293T cells were transiently transfected with equivalent amounts of plasmid and harvested under identical conditions. Protein levels were assessed by western blotting with endogenous GAPDH as a loading control.
(B) Full length PASD1 interacts with CLOCK and/or BMAL1 when they are co-expressed, but the isolated PASD1 N-terminus cannot. HEK293T cells were transfected with the indicated plasmids and proteins were co-precipitated using FLAG affinity resin. The N-terminal construct (residues 1 – 311) contains the PAS-A domain of PASD1 and lacks the CC1 domain. Due to interference of the IgG (*) with the band for MYC-PASD1ΔCC1, the C-terminal construct was used to assess the effect of deletion of the CC1 domain on interaction with CLOCK and BMAL1 (see Fig. 3E).
(C) CLOCK and BMAL1 mutants show decreased activity compared with wild-type CLOCK:BMAL1 complex but are active over the background of *Per1:luc* reporter. HEK293T cells were transfected with equivalent amounts of CLOCK and BMAL1 plasmids in the following combinations to yield activity over background: CLOCK:BMAL1, ~30-fold activation; CLOCK HI:BMAL1 LL/AA, ~12-fold activation; and CLOCKΔ19:BMAL1,~3-4-fold activation. Raw luminescence counts from one representative assay (in triplicate) are shown ± SD.

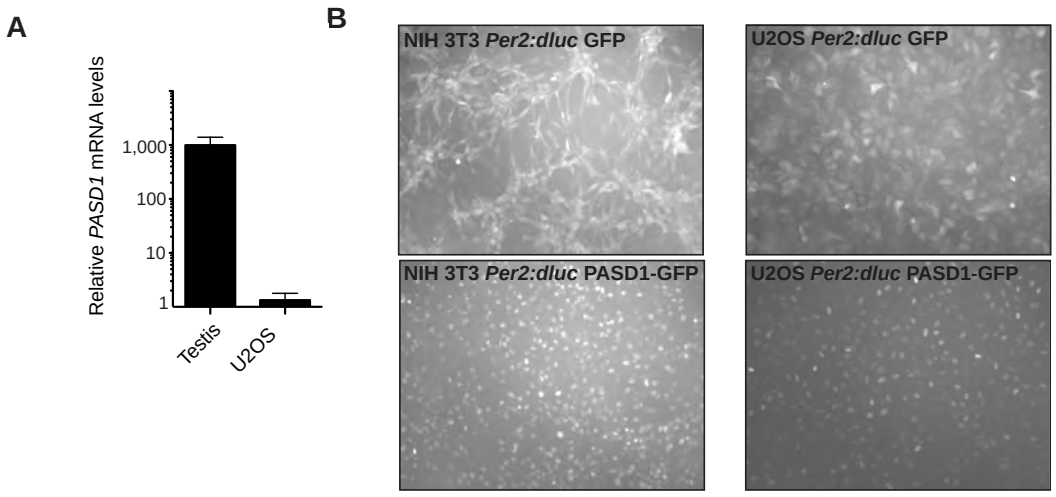

Figure S4. Validation of reagents used in PASD1 overexpression studies. (related to Figure 4)
(A) Comparison of *PASD1* expression in human testis and U2OS cells by RT-qPCR. U2OS cells exhibit > 0.2% relative *PASD1* mRNA abundance compared to expression in human testis, which is normalized to 1. Data are duplicated from Fig. 4A (linear y-axis) and shown in log10 format to illustrate the difference in *PASD1* expression.
(B) Representative images of GFP-positive cells taken immediately before bioluminescence recording of circadian rhythms. GFP-positive cells were sorted using fluorescence-activated flow cytometry and plated at 90-100% confluency 24 hours prior to recording.

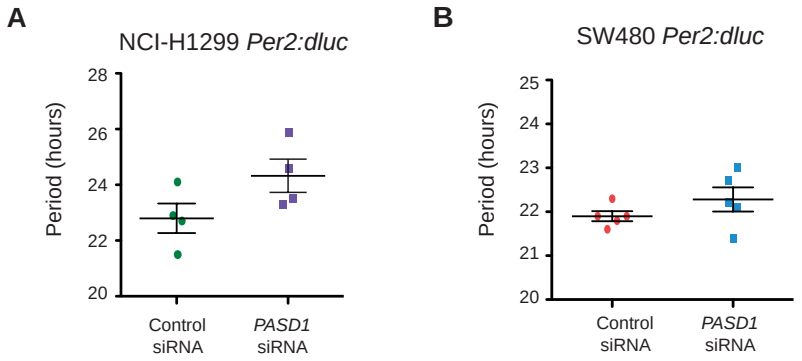

C

	Period (hours ± SEM)	
NCI-H1299 *Per2:dluc*		
Control siRNA	22.80 ± 0.53	p = 0.1054
PASD1 siRNA	24.33 ± 0.59	
SW480 *Per2:dluc*		
Control siRNA	21.90 ± 0.12	p = 0.2371
PASD1 siRNA	22.28 ± 0.27	

Figure S5. Knockdown of *PASD1* in cancer cell lines shows a trend towards lengthened period. (related to Figure 6)

(A) NCI-H1299 *Per2:dluc* and (B) SW480 *Per2:dluc* cells transfected with *PASD1* siRNA show a trend towards lengthened period. Data represented 4 or 5 independent runs with mean ± SEM plotted.

(C) Quantification of circadian periods in the two cell lines with statistical assessment. Statistical significance was assessed by Student's t-test (unpaired, two-tailed).

Table S1. Oligonucleotides for qPCR (related to Figure 5)

SYBR	5’ – 3’
Human beta actin (hACTB) FOR	CATGTACGTTGCTATCCAGGC
Human beta actin (hACTB) REV	CTCCTTAATGTCACGCACGAT
Human PASD1 FOR	TCCAGAGAGCAGGCTGAACAA
Human PASD1 REV	AAGCCGGATGTAATCCTGTG
Human BMAL1 FOR PrimerBank ID: 71852581c3	CATTAAGAGGTGCCACCAATCC
Human BMAL1 REV	TCATTCTGGCTGTAGTTGAGGA
Human GAPDH FOR	CATCAATGGAAATCCCATCA
Human GAPDH REV	TTCTCCATGGTGGTGAAGAC
Taqman	
PASD1 Exon 11 – 12 region	Hs01098424_m1
PASD1 Exon 14-15	Hs00542871_m1

Table S2. siRNA sequences (related to Figure 6)

siRNA sequences	5’ – 3’
Scramble control	GAAGCCCATTTAGATACCTCATGAT
PASD1 S1	TCAACCAAGTGACGCTACAGTTATT
PASD1 S2	TCCTGTGGTCTTTAGTGGCTTGTTT

*100nM of Scramble control and 50nM of PASD1 S1 with 50nM PASD1 S2

Supplemental Experimental Procedures

Transient transfection and reporter assays

For *Per1*:*luc* reporter gene assays, plasmids were transfected in duplicate into HEK293T cells in a 48-well plate using LT-1 transfection reagent (Mirus) with the indicated plasmids: 5 ng pGL3 *Per1:luc* reporter, 100 ng each pSG5-BMAL1 and pSG5-CLOCK. Full-length cDNA for human PASD1 (accession # BC040301.1; Open Biosystems) was validated by complete sequencing. Amounts of pcDNA4B- His_6MYC-FLAG-CRY1 and pcDNA4B His_6MYC-PASD1 used were as follows: 1, 5 and 50 ng of plasmid were used in the titration of CRY1 and PASD1v2, and 50, 100 and 200 ng of plasmid were used in the titration of PASD1 (aa 1-638) and PASD1ΔCC1 (aa 1-638 with deletion of aa 315-465); in all cases, empty pcDNA4B vector was used to normalize total plasmid to 800 ng/well. For full-length PASD1 (aa1-773) and PASD1 C-term (312-773), 10 or 100 ng were transfected for each construct. Cells were harvested 30 hours after transfection using Passive Lysis Buffer (NEB) and luciferase activity assayed with Bright-Glo luciferin reagent (Promega) on a Perkin Elmer EnVision plate reader. Each reporter assay was repeated at least three independent times.

Co-immunoprecipitations

HEK293T cells (ATCC) were grown in DMEM supplemented with 10% fetal bovine serum. Cells were transfected using the calcium phosphate method with plasmids expressing His_6FLAG-CLOCK (pSG5-CLOCK), FLAG-BMAL1 (pSG5-BMAL1) and His_6MYC-tagged truncations of pCDNA4B-PASD1 as follows: PASD1 (aa 1-638), C-term (aa 312-638), C-termΔCC1 (aa 312-638), N-term (aa 1-311) as indicated. Cells were seeded into 60 mm dishes (750,000 cells) 16 hours prior to transfection. Approximately 24 hours post-transfection, cells were incubated on ice for 10 min. in PASD1 lysis buffer (20 mM HEPES-KOH pH 7.5, 100 mM NaCl, 1 mM EDTA, 1% Triton X-100, 5% glycerol), then sonicated briefly

(~2 sec) on low power to extract proteins from chromatin. Extracts were clarified by centrifugation at 13.2K rpm for 10 min. at 4°C. 25 µL of clarified extract was removed for input sample. The remaining extract was added to 300 µL lysis buffer containing 15 µl anti-Flag M2 affinity resin (Sigma). Tubes were rotated end over end for 4 hours, and resin was washed three times with 400 µL lysis buffer. Proteins were eluted from resin by addition of 30 µL 2X SDS Laemmli buffer containing 1% β-mercaptoethanol and boiled for 4 minutes. Proteins were resolved by standard SDS-PAGE (7.5% gel, BioRad) and transferred to 0.45 µm nitrocellulose membrane (BioRad). Membranes were blocked with 5% (w/v) non-fat milk in Tris-buffered saline with Tween-20 (TBST; 20 mM Tris pH 7.5, 150 mM NaCl, 0.1% (v/v) Tween-20) and probed with anti-FLAG (1:2,000; Sigma-Aldrich) or anti-MYC (1:2,500; 9E10 ascites fluid, University of Iowa Developmental Studies Hybridoma Bank, DSHB). HRP-conjugated secondary antibodies were used at 1:10,000 (Santa Cruz Biotechnology) in TBST. Western signal was detected using Clarity ECL reagent (Bio-Rad) and visualized on a ChemiDoc XRS+ imager (Bio-Rad).

For endogenous co-immunoprecipitations from nuclear extract, approximately 1 x 10^8 U2OS PASD1-GFP or NCI-H1299 cells were lysed in hypotonic lysis buffer (10 mM HEPES-KOH pH 7.5, 10 mM KCl, 1.5 mM $MgCl_2$, 340 mM sucrose, 10% glycerol, 0.1% Triton X-100) containing 1x protease inhibitor cocktail (Roche). Nuclei were pelleted by centrifugation at 4K rpm for 5 min at 4°C, washed once with hypotonic lysis buffer, then resuspended in PASD1 lysis buffer (20 mM HEPES-KOH [7.5], 100 mM NaCl, 1 mM EDTA, 1% Triton X-100, 5% glycerol) containing 1x EDTA-free protease inhibitor cocktail (Roche) and 1 mM PMSF. Lysates were incubated on ice for 10 min, sonicated briefly on low power, then centrifuged at 13.2K rpm for 10 min at 4°C. Cell lysates were incubated with 4 µg of rabbit normal IgG (Santa Cruz Biotechnology), CLOCK (H-276; Santa Cruz Biotechnology), BMAL1 or rPASD1 antibody for 2 hours at 4°C, followed by incubation with 15 µL protein A/G agarose (Pierce) overnight at 4°C. IPs were washed three times with PASD1 lysis buffer containing 0.05% Triton X-100 and once with lysis buffer without Triton X-100. Samples were boiled in SDS sample

buffer containing 5% β-mercaptoethanol and 50 mM DTT. Proteins were resolved by standard SDS-PAGE (7.5% gel, BioRad) and transferred to 0.45 µm nitrocellulose membrane (BioRad). Membranes were blocked with 5% non-fat milk/TBST and probed with anti-CLOCK (1:250; S-19, SCBT), anti-BMAL1 (1:250; B-1, SCBT), or anti-PASD1 (1:100; PASD1-2) antibodies in 2.5% non-fat milk/TBST. HRP-conjugated secondary antibodies were used at 1:10,000 (SCBT) in 2.5% non-fat milk/TBST.

Lentiviral constructs and production

NIH3T3, U2OS, NCI-H1299 and SW480 cells (ATCC) were first infected with pLV7-Bsd-P(Per2)-dLuc reporter (a kind gift from Andrew Liu, University of Memphis) followed by blasticidin selection to generate stable reporter cell lines. For overexpression studies in U2OS and NIH3T3 *Per2:dLuc* cells, PASD1-EGFP (PASD1, aa 1-773) and EGFP constructs were cloned into the pCDH-neo-514B-1 lentiviral vector (Systems Biosciences). Third-generation lentiviruses were generated by transient co-transfection of HEK293T cells with a four-plasmid combination as follows: one 150 mm dish containing 1.0 x 10^7 293T cells was transfected using the calcium phosphate method with 40 µg lentiviral vector, 20 µg pMDLg/pRRE (Addgene, #12251), 10 µg pRSV-Rev (Addgene #12253) and 12 µg pMD2.G (Addgene, #12259). Supernatants were collected 48 hours after transfection and lentiviral particles were concentrated using PEG-IT (Systems Biosciences) according to the manufacturer's protocol.

Lentiviral transduction

NIH3T3 and U2OS cells were grown to ~60 - 70% confluency in 60 mm dishes and infected with EGFP or PASD1-EGFP lentiviral particles to obtain a multiplicity of infection (MOI) of 1 using 8 µg/mL polybrene (Santa Cruz Biotechnology). When cultures reached confluency, cells were trypsinized, expanded and subjected to 400 µg/mL G418. After approximately one week of antibiotic selection (determined by the kill curve of mock-infected cells), cells were sorted for GFP positive cells by FACS using the FITC channel (BD

FACSAria II Cell Sorter) to obtain a pure transgene positive population. Immediately after sorting, cells were plated for bioluminescence recording.

Bioluminescence recording and data analysis

Cell lines were generated as described above and were grown to 90 – 100% confluency under each condition in 35 mm dishes. After reaching appropriate confluency, cell culture media was replaced with HEPES-buffered phenol-free DMEM media containing 100 nM dexamethasone and 100 µM D-luciferin. Dishes were covered with 40 mm glass coverslips (Fisher Scientific) and sealed with vacuum grease to prevent evaporation. Emission of bioluminescence from reporter cells was monitored at 37°C without added CO_2 using a LumiCycle luminometer (Actimetrics). Dominant circadian period, amplitude and damping were extracted using the accompanying LumiCycle software and fit using the dampened sinusoidal waveform. In all bioluminescence traces, the data shown are representative from greater than three independent experiments (on average, n = 8-11).

siRNA-mediated PASD1 knockdown

NCI-H1299 *Per2:dluc* and SW480 *Per2:dluc* cells were grown to ~70% confluency in 35 or 60 mm dishes. Cells were transfected with siRNA duplexes at 100nM final concentration using Lipofectamine 2000 according to the manufacturer's protocol. After 72 hours of incubation with siRNA, mRNA was isolated from 60 mm dishes and subject to RT-qPCR or 35 mm dishes were prepared for bioluminescence recording. To visualize PASD1 protein knockdown by western blot, 1.5 x 10^6 NCI-H1299 *Per2:dluc* cells were transfected with siRNA as described above and the cells were lysed in 150 µL PASD1 lysis buffer after 72 hours incubation time as described above. 50 µg total protein was resolved by standard SDS-PAGE (7.5% gel, BioRad) and transferred to 0.45 µm nitrocellulose membrane (BioRad). Membranes were blocked with 5% non-fat

milk/TBST and probed with anti-rPASD1 (1:500) in 2.5% (w/v) non-fat milk/TBST. HRP-conjugated secondary antibodies were used at 1:10,000 (SCBT) in 2.5% (w/v) non-fat milk/TBST.

Reverse transcription and qPCR

To assess *PASD1* mRNA knockdown after siRNA treatment in NCI-H1299 *Per2:dluc* and SW480 *Per2:dluc, t*otal RNA was isolated from cells using TRIzol reagent according to the manufacturer's instructions (Life Technologies) with the following modifications: after precipitation with isopropanol, the pellet was resuspended in 360 µL SDS extraction buffer (20 mM Tris-HCl pH 7.5, 1 mM EDTA, 0.5% (w/v) SDS). After resuspending the pellet, 0.1 volume of 3 M NaOAc (pH 5.3) and 200 µL phenol:chloroform:isoamyl alcohol were added and centrifuged at 12,000g for 15 min. at 4°C in a phase lock tube (5 Prime). RNA was then washed with 75% ethanol and resuspended in RNAse free water. RNA was treated with TURBO DNA-free kit (Life Technologies). For analysis of transcripts, 1 µg total RNA was reverse transcribed using the iScript kit (BioRad). cDNA reactions were diluted 1:10 and 4 µL of cDNA dilution were used for qPCR (20 µL reaction volume). qPCR reactions were performed using iTaq SYBR Green supermix (BioRad) in a 96-well plate format on a BioRad CFX Connect instrument. Transcript levels were normalized to human *ACTB and GAPDH*. *ACTB*: 250nM, 250 bp amplicon; *PASD1*: 250nM, 238 bp amplicon; *BMAL1*: 250nM, 187bp amplicon; *GAPDH*: 250nM, 140 bp amplicon.

For RT-qPCR performed on the panel of cancer cell lines, total RNA was extracted using QIAgen's RNeasy Mini kit. For analysis of transcripts, 500 ng of total RNA was used for cDNA synthesis with 100 ng random primers (Promega) and 100U Superscript III (Invitrogen) in a 20 µL reaction. cDNAs were diluted 1:5 and 4 µL of the diluted cDNAs were used for qPCR (20 µL reaction volume). qPCR was performed using 2 TaqMan assays for PASD1 and EXPRESS qPCR Supermix (Invitrogen) on Chromo4 Real-Time Detector (Biorad). Human testis

total RNA samples were purchased from: Takara-Clontech (Saint-Germain-en-Laye, France), Ambion (via Invitrogen; Paisley, UK) and Agilent (Stockport UK).

Immunohistochemistry

Formalin-fixed paraffin-embedded cell pellets were prepared by fixing cells in formalin for 24 hours then processing and embedding in paraffin according to standard histological procedures. 4 µm sections were dewaxed, rehydrated and then subjected to pressure cooker antigen retrieval in 50 mM Tris pH 9, 2 mM EDTA for 2 minutes and then incubated with the PASD1-1 monoclonal antibody, or negative control antibody, at a dilution of 1:60 for 2 hours at room temperature. Labeling was detected using the Novocastra Novolink™ Polymer Detection System (Leica Biosystems, Newcastle, UK).

Western blotting

For western blotting of the panel of cancer cell lines, lysates were prepared using Mammalian Protein Extraction reagent containing Universal Nuclease (Pierce). 30 µg whole cell lysates were resolved on 7.5% acrylamide gel and transferred to Protran nitrocellulose membrane (GE Healthcare). Membranes were blocked in 5% (w/v) low fat milk in 1X PBS for 1 hour at RT, and were then incubated with primary antibodies overnight at 4°C diluted in 5% (w/v) low fat milk in PBS at the following concentrations: 1:10 PASD1-1; 1:10 PASD1-2, or 1:20,000 anti-β-Actin (Sigma, clone AC-15). IgG-HRP secondary antibodies (Dako) were diluted 1:5,000 in 5% low-fat milk/PBS and visualized with ECL reagent (GE Healthcare).